



Scanning Near-Field Optical Microscopy: Relevant Insights and Trends

Shelaev Artem, application scientist
shelaev@ntmdt-si.com

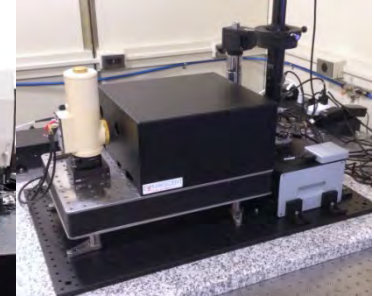


Product Line

AFM



AFM-Raman / TERS / SNOM



SOLVER NANO

NEXT / TITANIUM

NTEGRA

NTEGRA SPECTRA II

NTEGRA IR

- Compact desktop AFM/STM for both education and science
- Full set of AFM/STM modes
- High AFM/STM performance
- Closed-loop Scanner

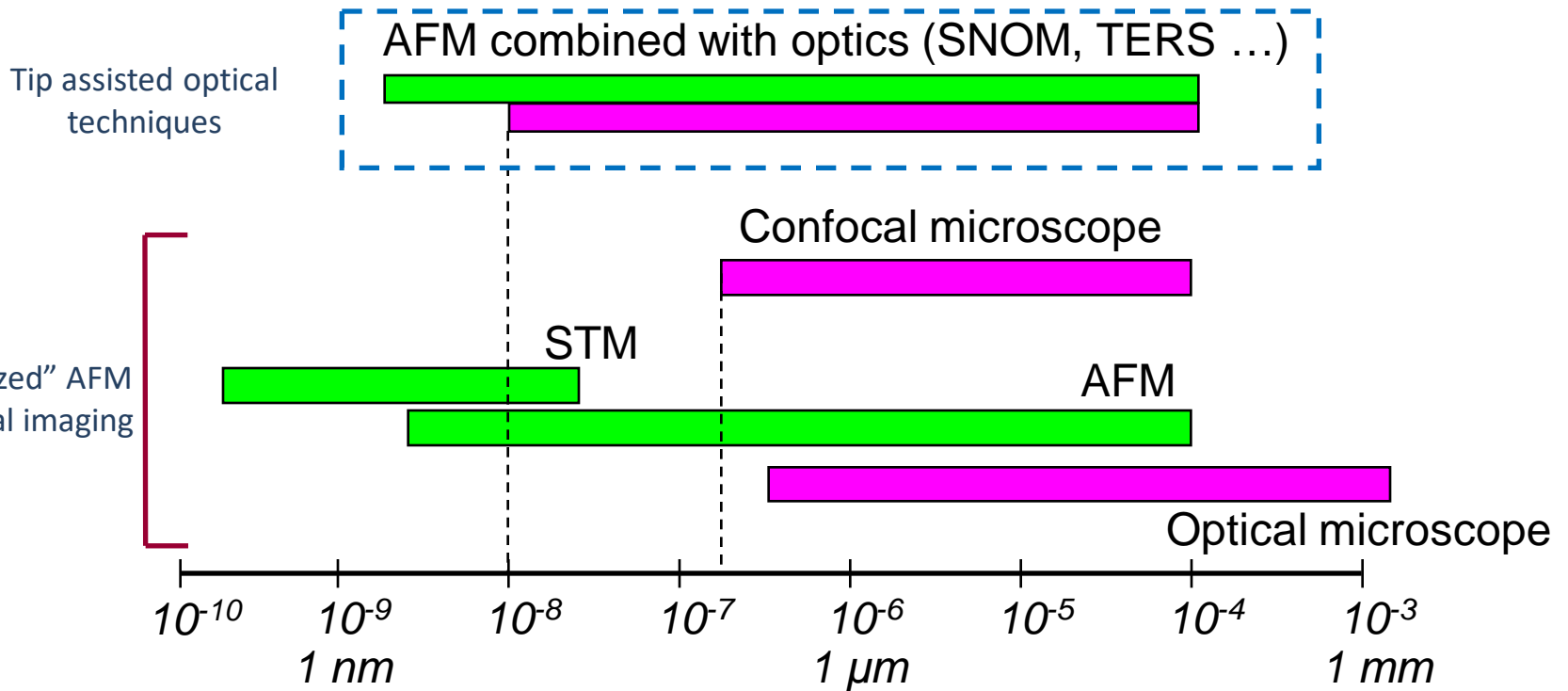
- AFM/STM with exceptional level of automation
- Fast, precise and low-noise closed-loop scanner
- High resolution imaging due to extremely low noise and high stability
- Full set of standard and advanced AFM/STM modes
- Hybrid Mode™

- Modular high performance AFM/STM for wide range of applications
- Fiber based SNOM
- Low noise and high resolution
- Full set of standard and advanced AFM/STM modes
- Hybrid Mode™

- SPM
- Automated AFM laser, probe and photodiode
- Confocal Raman / Fluorescence / Rayleigh Microscopy
- Aperture SNOM
- Tip Enhanced Raman Scattering (TERS)
- TERS optimized system for all possible excitation/detection geometries
- Hybrid Mode™

- IR sSNOM system
- High resolution AFM
- Stabilized CO₂ laser
- Hybrid Mode™

Resolution and capabilities of different techniques



Optical techniques (color imaging, physical & chemical analysis)

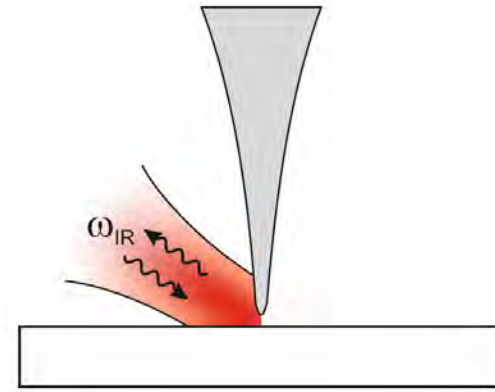
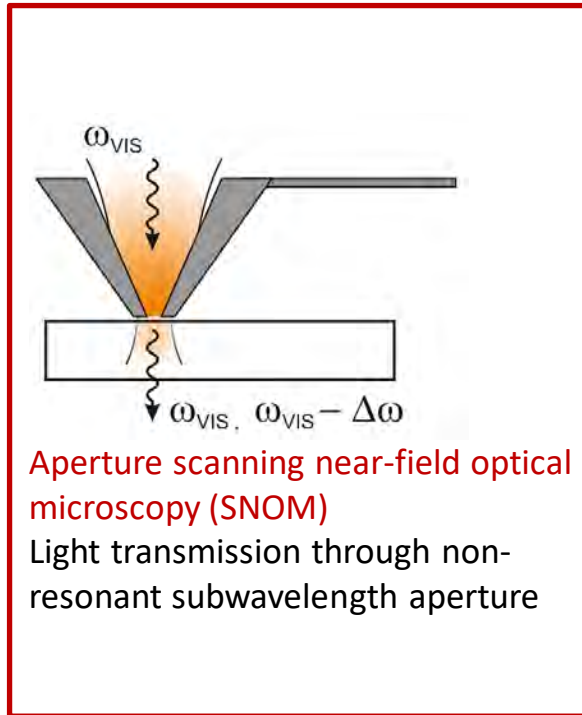


Scanning probe microscopy (topography, mechanical, electrical, magnetic and other properties of the surface)



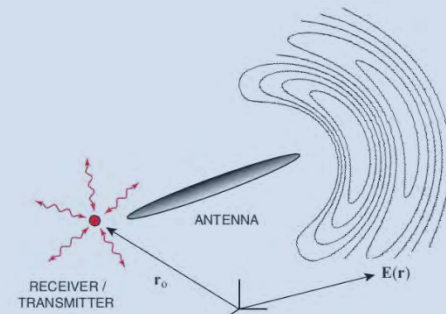
AFM (STM) + Optical techniques = Dramatic increase of resolution and sensitivity

Super-resolution imaging using scanning optical antennas



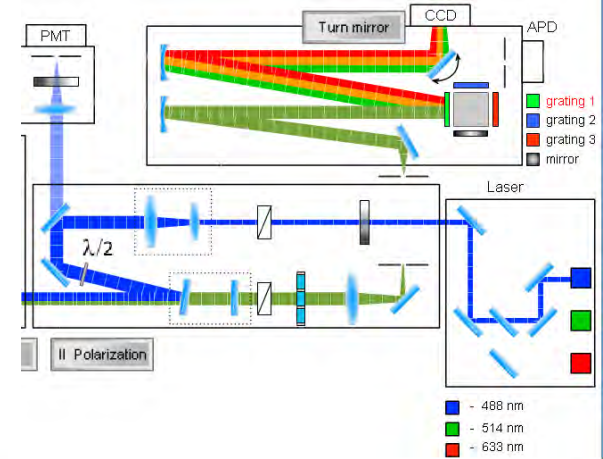
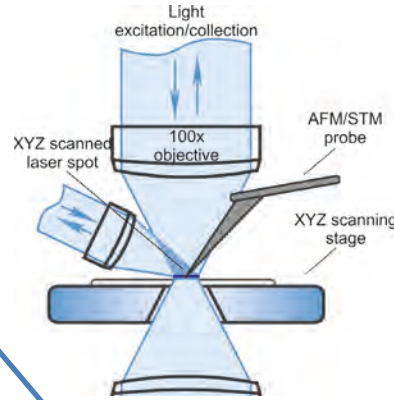
Optical antenna: a device designed to efficiently convert free-propagating optical radiation to localized energy, and vice versa.

- L. Novotny, N. van Hulst, *Nature photonics* 5, 89 (2011)
- P. Bharadwaj, B. Deutch, L. Novotny, *Adv. In Opt. Phot.* 1, 438 (2009)
- Pohl D. W., *Optics, Principles and Applications* (World Scientific, 2000).





Upright, Inverted and Side illumination configuration



Light input from side (with scanning mirror)

Top optics (LED illuminator & camera)

Light input from top (with scanning mirror)

Optical AFM (AFM probe + 100x objective on the top)

XYZ sample stage (bottom illumination objective inside)

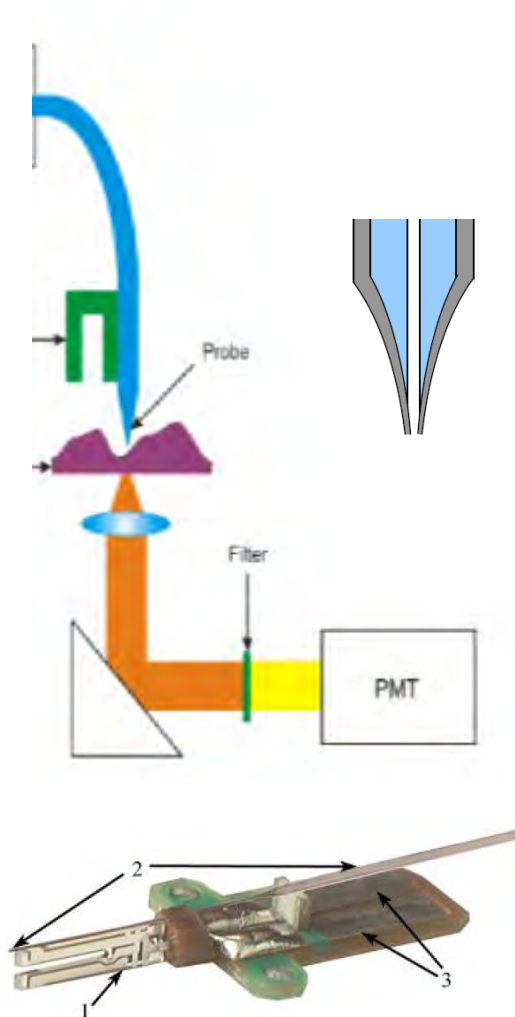
Light input from bottom (with scanning mirror)

Bottom optics (LED illuminator & camera)

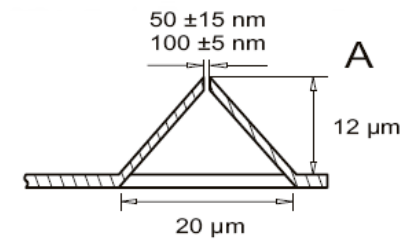
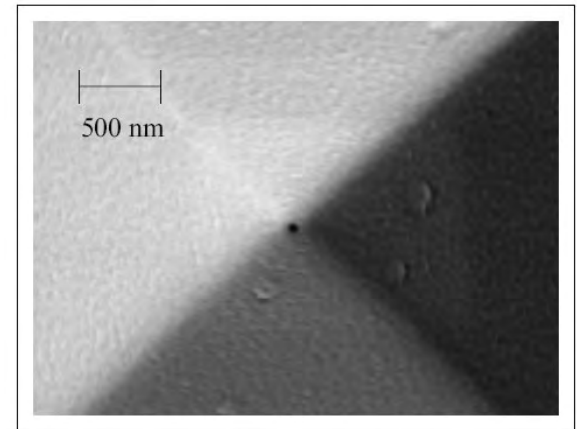
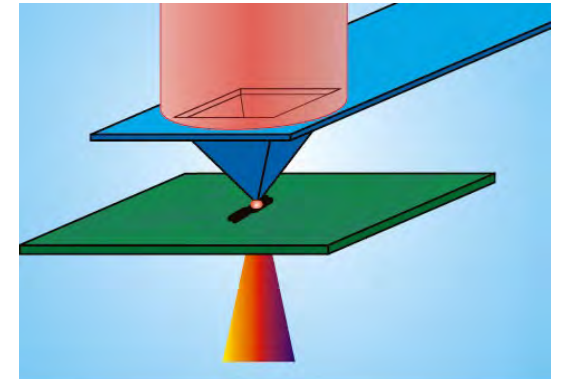


ALL types of SNOM probes

1. Straight quartz fiber (glued to tuning fork)

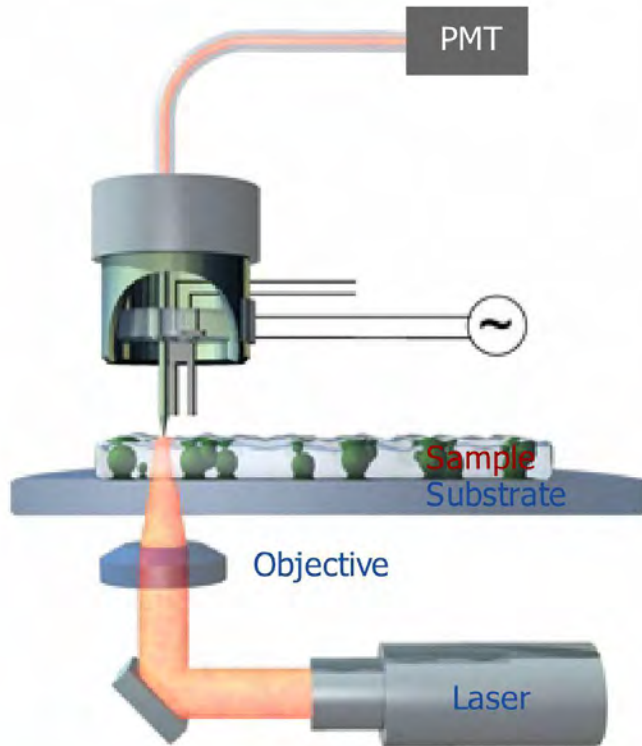


2. Silicon cantilevers with aperture



Two major types of aperture SNOM

FIBER SNOM

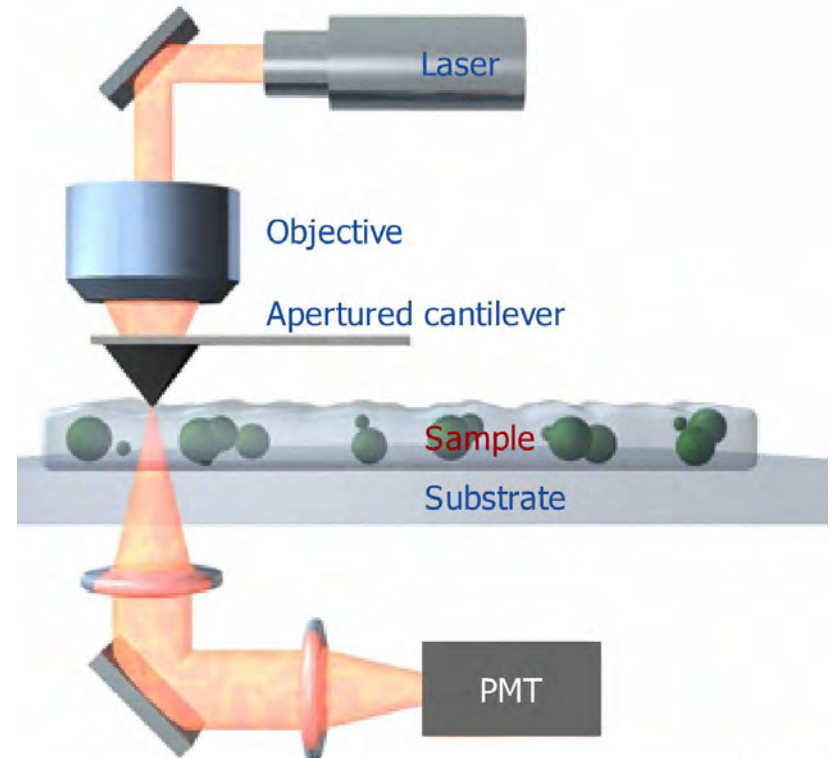


Copyright © NT-MDT

www.ntmdt.com

Example shows
SNOM collection mode
(laser signal)

CANTILEVER SNOM

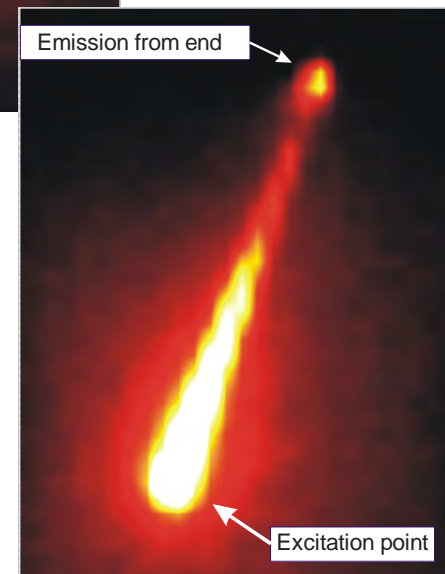
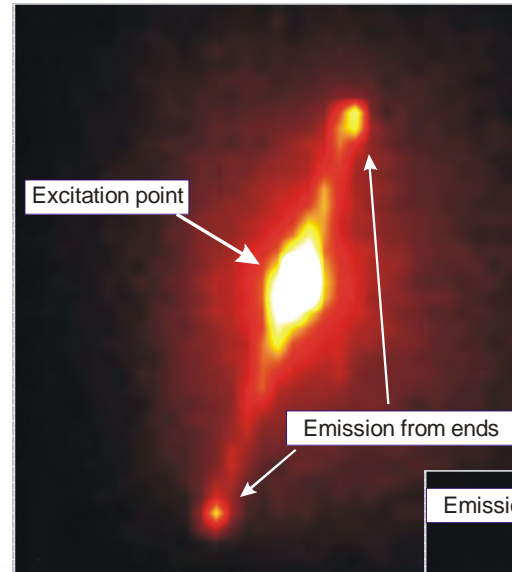
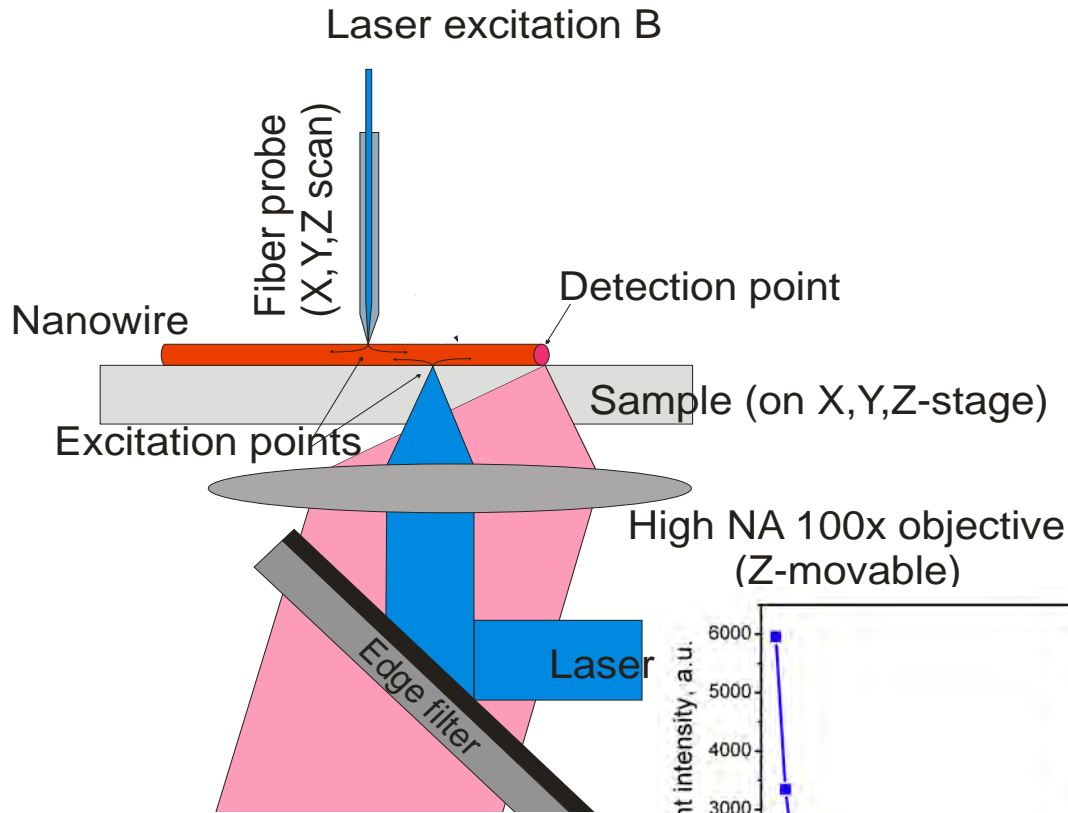


Copyright © NT-MDT

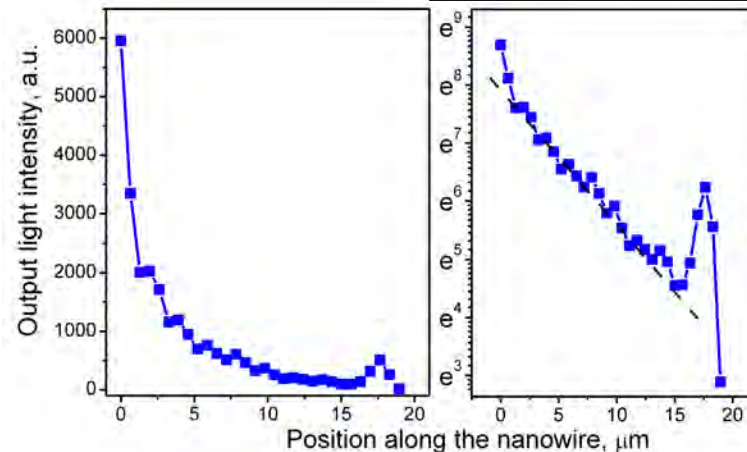
www.ntmdt.com

Example shows
SNOM Transmission mode
(laser signal)

Light Transport in Nanowires

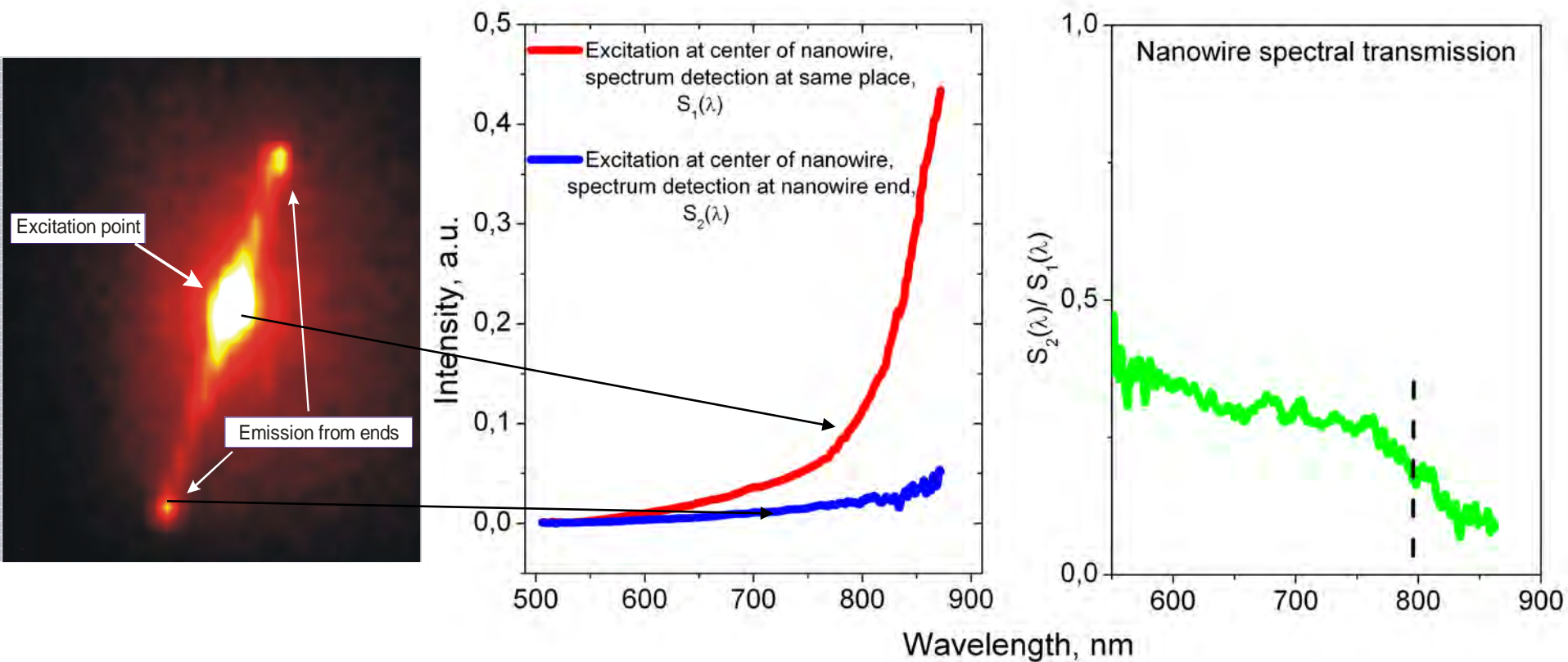


High NA 100x objective (Z-movable)



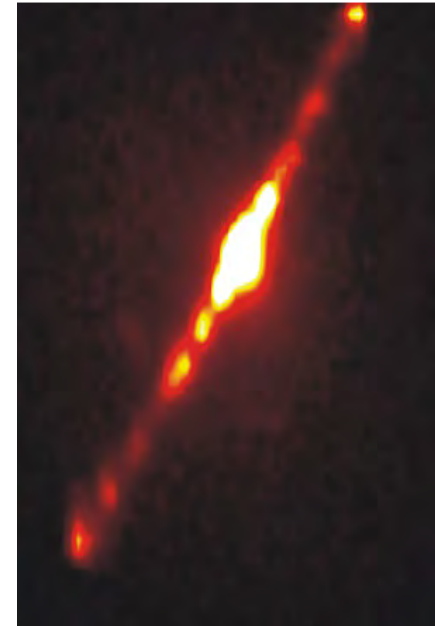
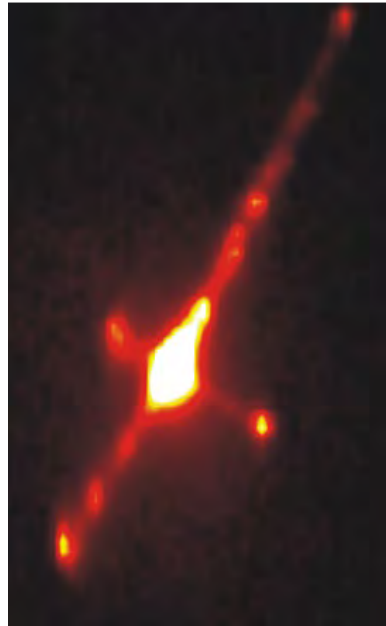
Nanowire is excited by 488 nm light at the body (left image) and at the left end (right image). Excitation green light is completely cut off from the image by two edge filters (with 10^{-6} transmission). Partly nanowire radiation ($>10\%$) is transmitted through the nanowire and is emitted from nanowire ends.

Light Transport in Nanowires



Nanowire is locally excited at the center. Red curve shows spectrum taken at the excitation point [in the middle of the nanowire]. Blue curve is the transmitted light spectrum taken at the nanowire end. Green curve shows spectral transmission function of the nanowire

Light Transport in Nanowires

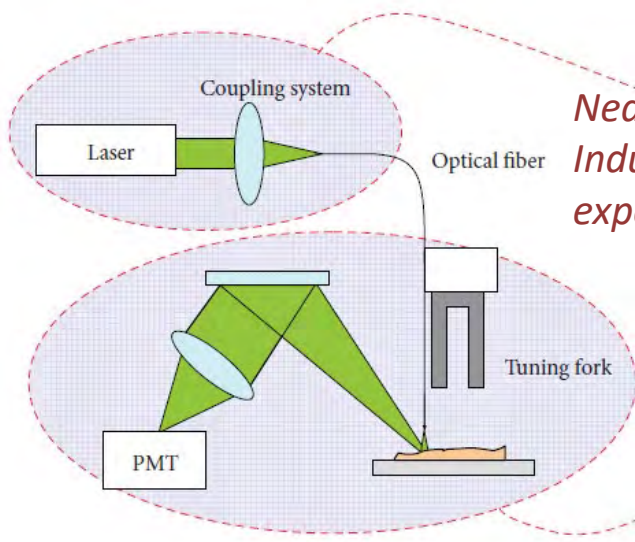
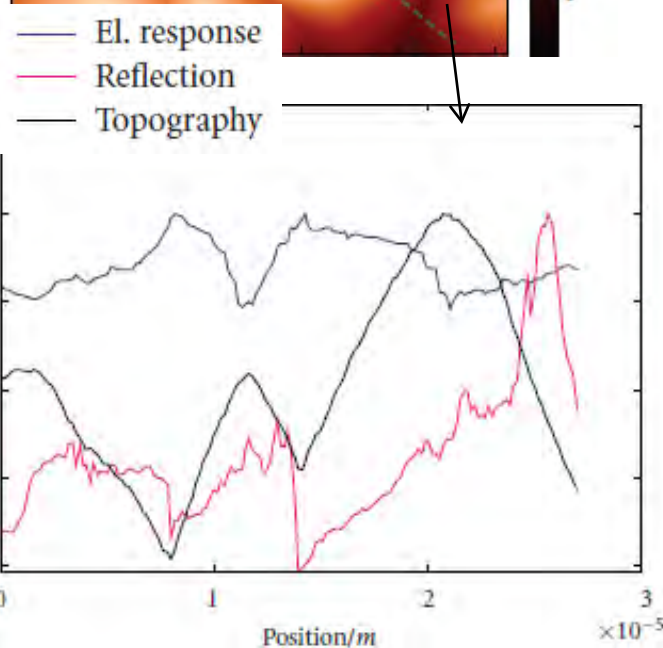
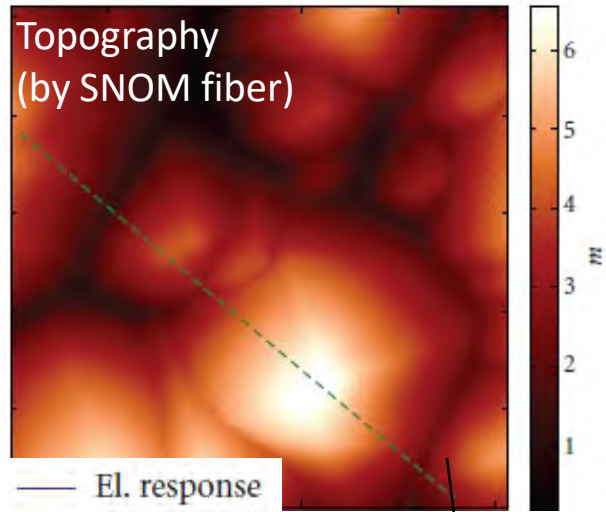


Light transfer through the nanowire containing large number of structural defects and crossing another nanowire.

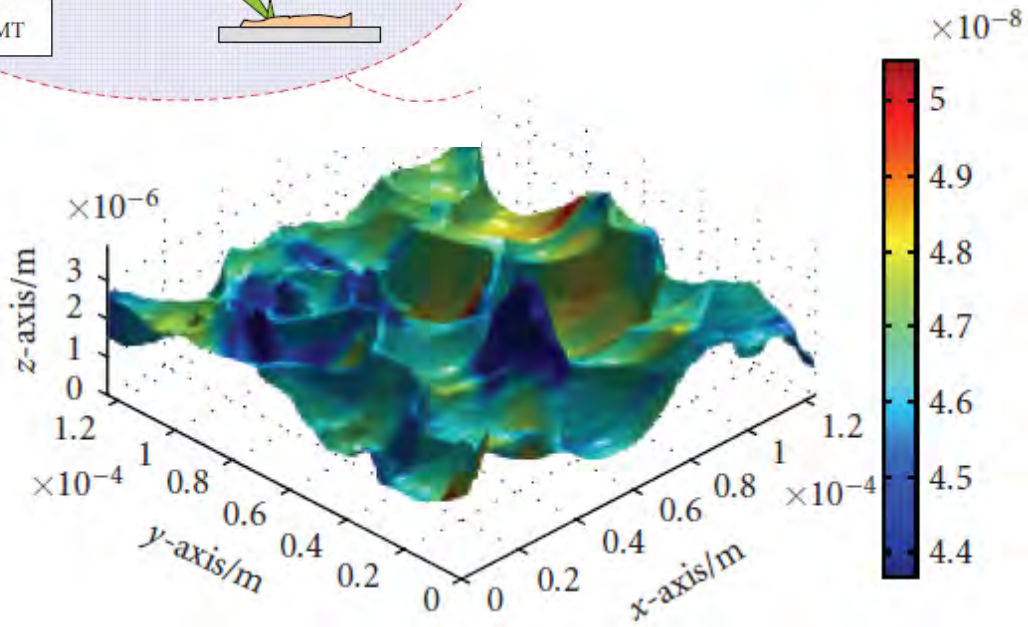
EASY EXPERIMENT – < 10 minutes for one nanowire



SNOM for localized optical excitation in photovoltaics



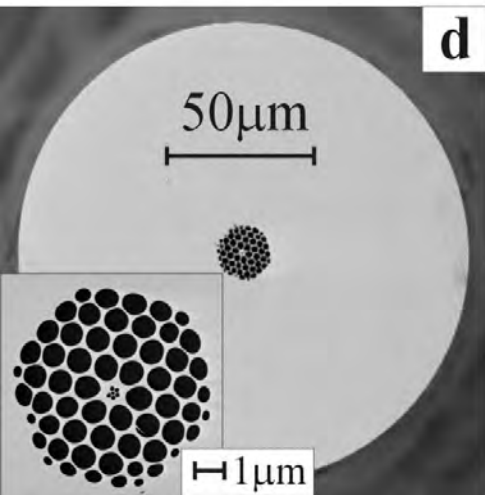
*Near-Field Optical Beam
Induced Photocurrent (NOB-IC)
experiment*



Overlay of topography (3D) and local light to current conversion coefficient (color)

Correlation of local reflectivity, local light-current conversion and topography

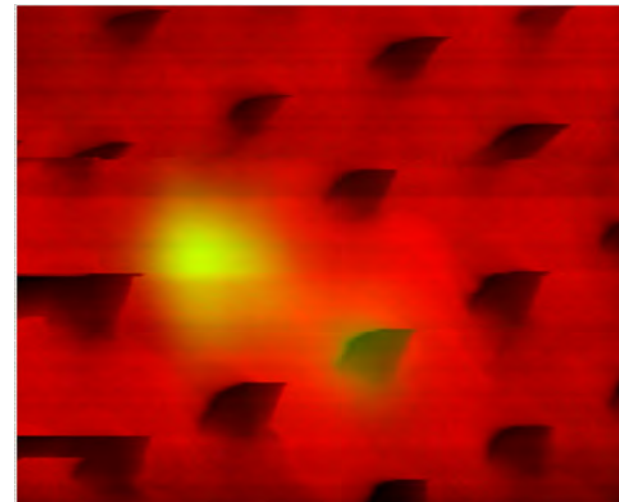
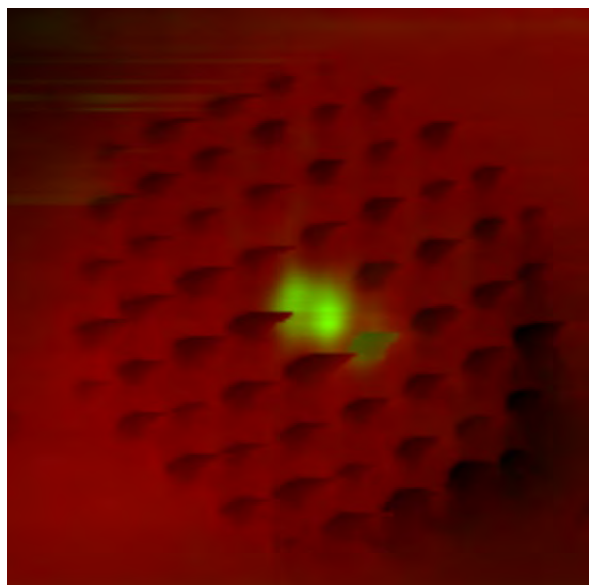
SNOM on photonic crystal optical fibers



SEM image of fiber cross-section



Launch light from outside of the NT-MDT system with particular sources



Overlay of simultaneously measured:
Sample topography (orange/red palette) and SNOM intensity (green palette)

Data courtesy:

Yinlan Ruan, Heike Ebendorff-Heidepriem,
Tanya M. Monro

Centre of Expertise in Photonics, School of Chemistry &
Physics, University of Adelaide, Adelaide, 5000 Australia

Focusing diffraction optical elements

Diffraction of a Gaussian beam by axicons is studied by SNOM. Binary diffraction axicons with the period close to the light wavelength are formed by electron beam lithography on a quartz substrate. Different axicon geometries are studied. It is shown experimentally that asymmetric microaxicon can reduce the spot size of central light beam along polarization direction in a near zone of diffraction – overcoming the diffraction limit.

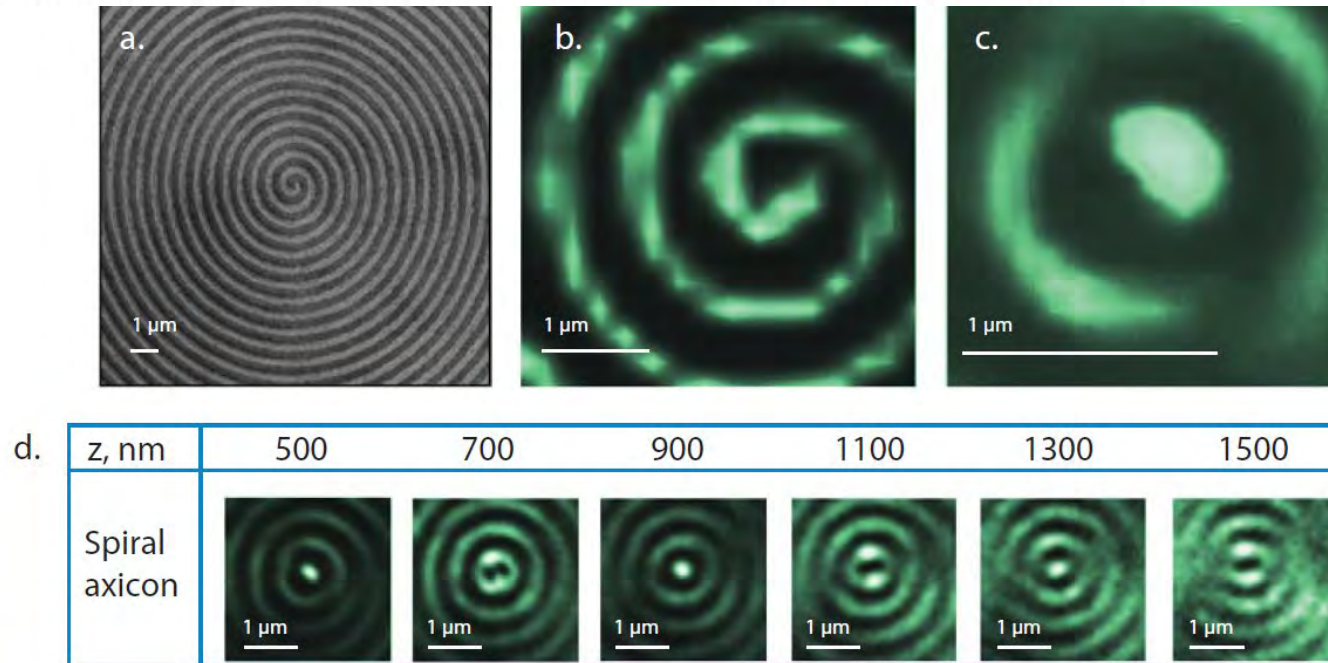
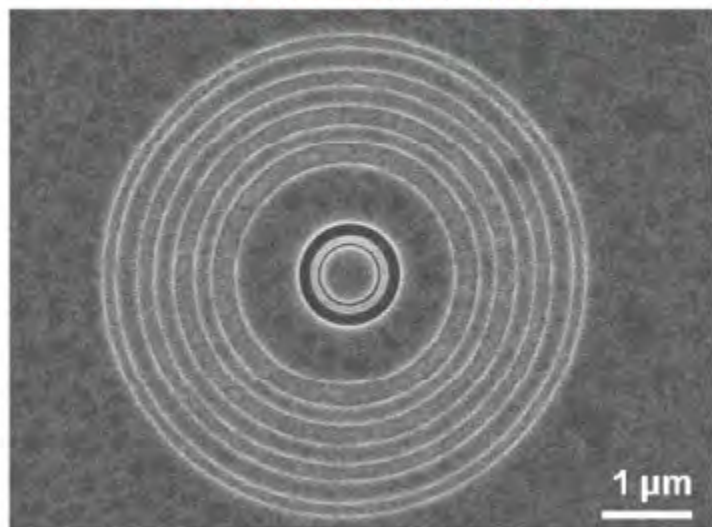


Fig. 7. (a) SEM image of the central part of a spiral axicon. (b) The diffracted light intensity distribution detected by SNOM in close proximity to the surface. (c) SNOM intensity distribution taken at ~ 500 nm from the surface. The central part of the beam at this plane is compressed in a light polarization direction (vertical) and has size less than optical limit. (d) Series of intensity distribution: the height of a scanning plane was varied from 500 nm to 1500 nm.

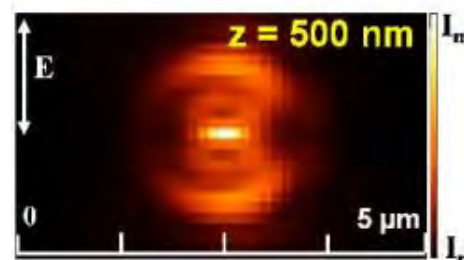
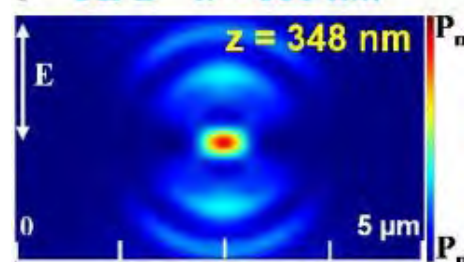
Data from: S. N. Khonina, D. V. Nesterenko, A. A. Morozov, R. V. Skidanov, and V. A. Soifer, *OPTICAL MEMORY AND NEURAL NETWORKS*, Vol. 21, No. 1, 17-26 (2012).

Focusing diffraction optical elements

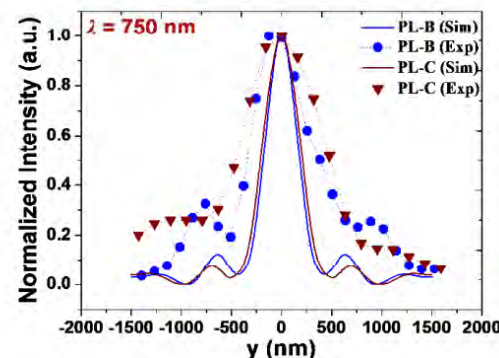
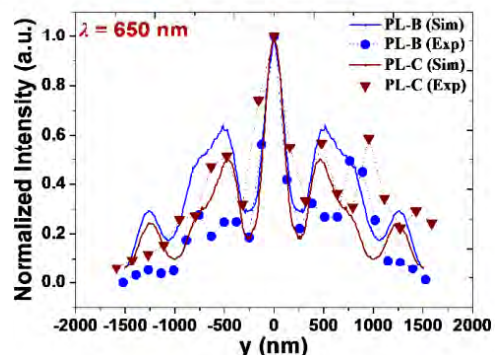
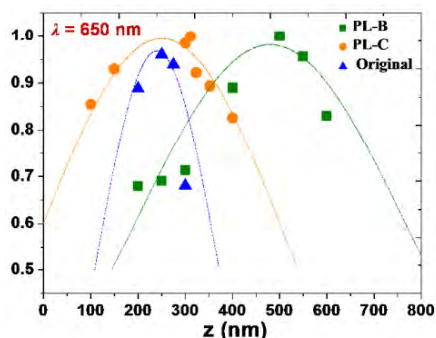
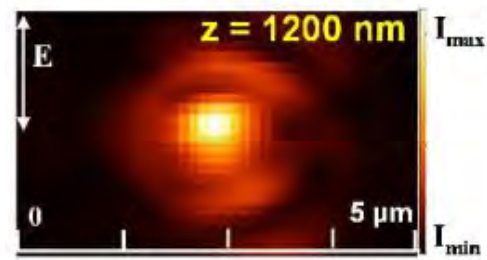
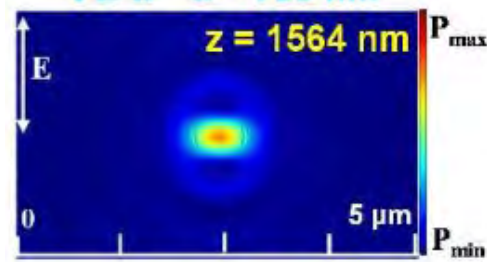
PL-B ($m = 1, 2, 3, 4$)



PL-B $\lambda = 650$ nm

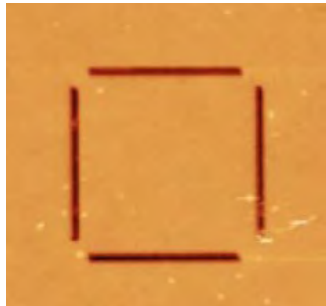


PL-B $\lambda = 750$ nm



SEM image and the measured power intensity distributions along the z-axis are shown for $\lambda = 650$ nm and $\lambda = 750$ nm. (c) The simulated and measured focal spots at each focal plane. (d) The measured and simulated power intensities along the y-axis show the narrower focal spot for the PL-B at both working wavelengths.

SPP interference studied by SNOM

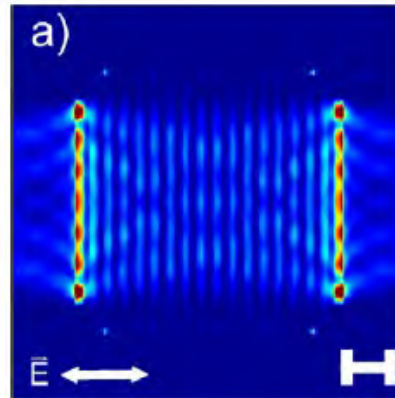


Slit structure in Au film (AFM image)

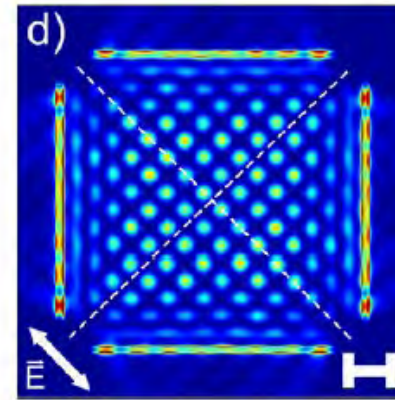
Excitation light polarization



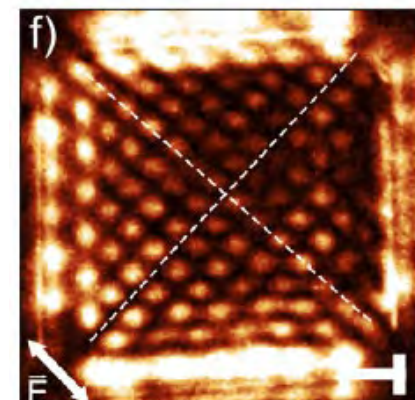
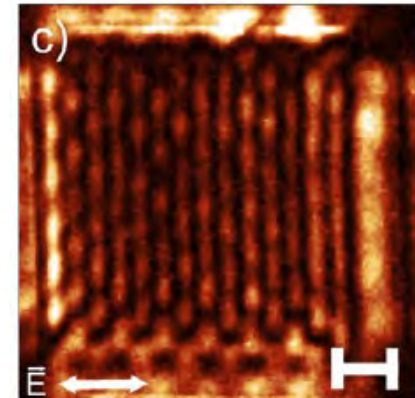
Numerical simulation



Excitation light polarization

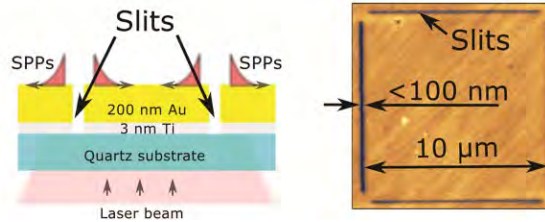
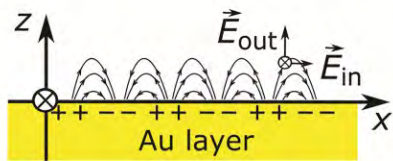
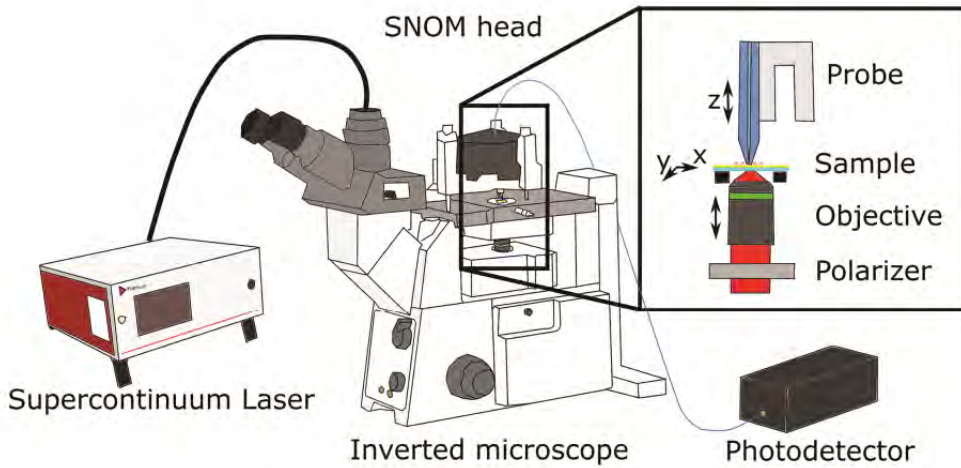


Experiment

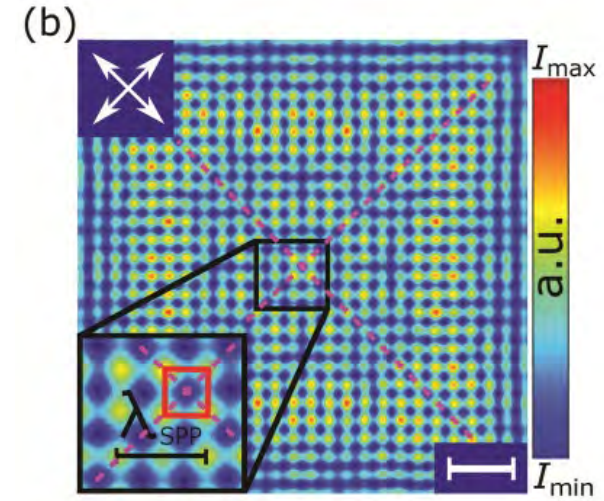


Near-field interference pattern of surface plasmon polaritons
in a square-like slit structure in Au film

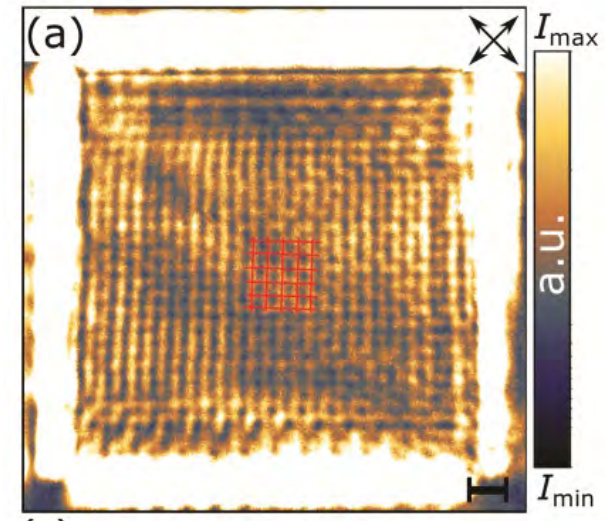
SPP interference studied by SNOM



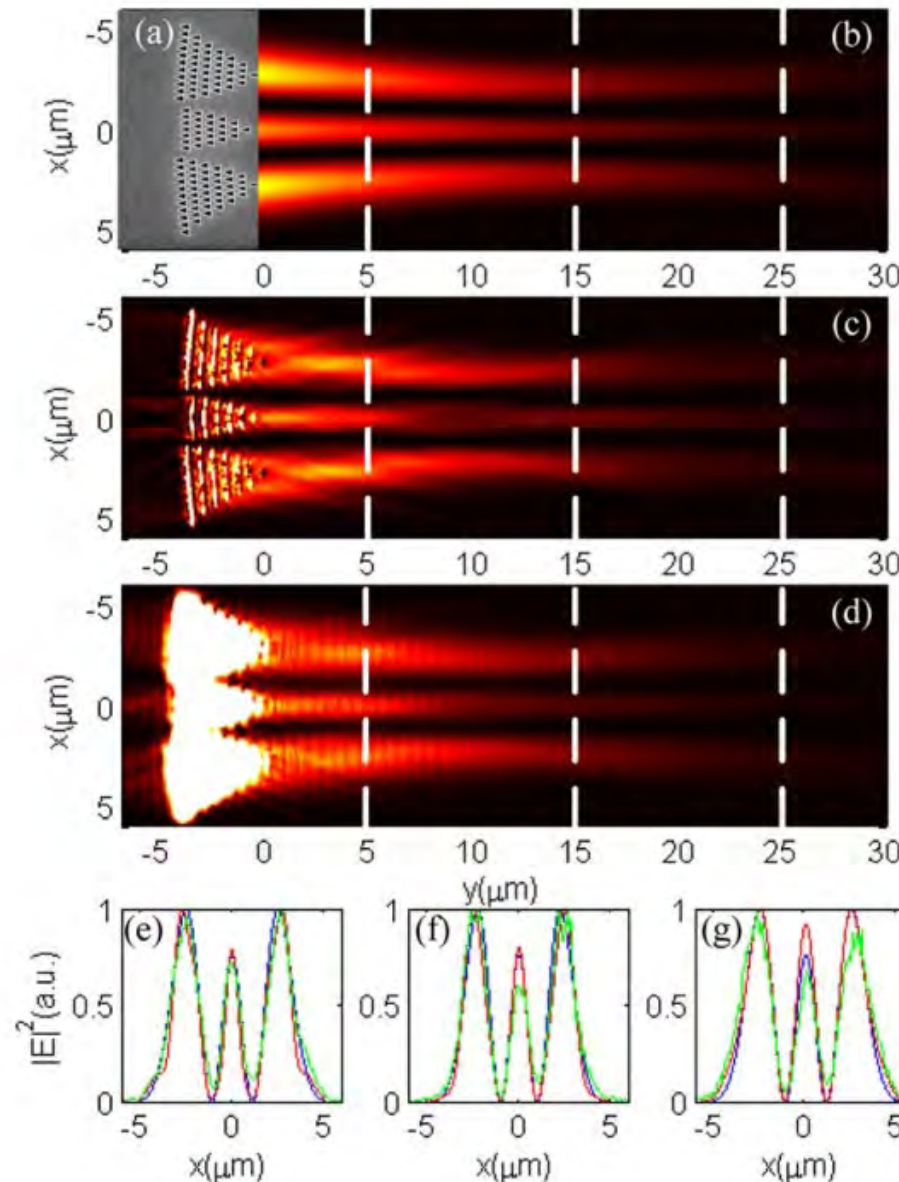
Numerical simulation



Experiment



Generating unidirectional SPP beams



Required shape

Numerical simulation for
calculated Delta-shape
structures

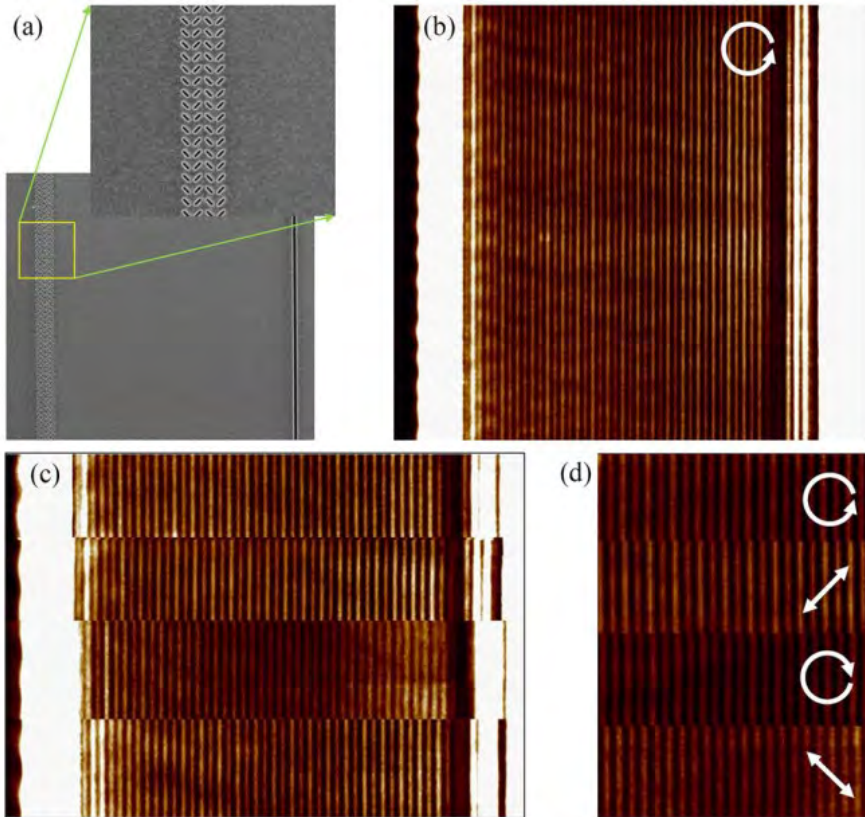
Experiment, SNOM data

Profiles at different
distances

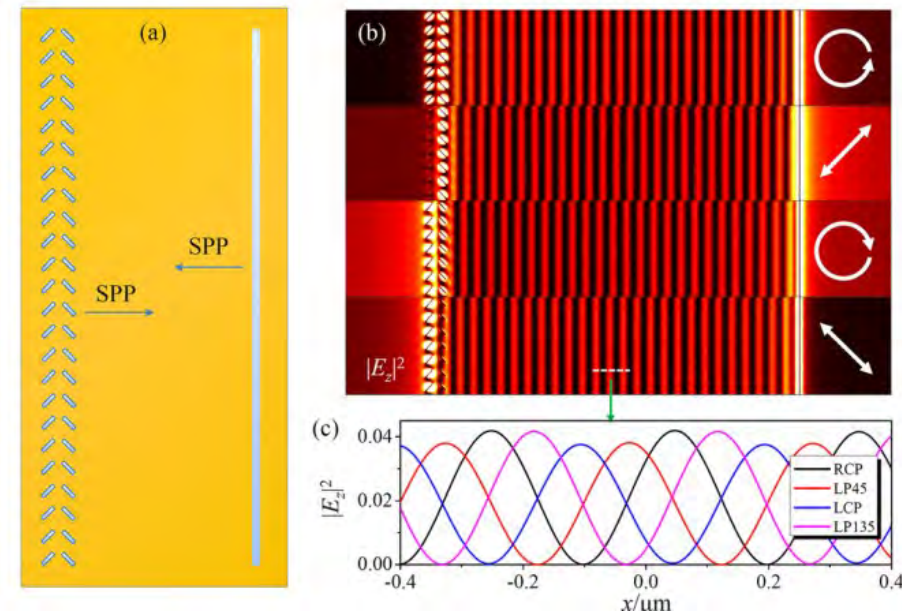
You, O., Wang, Q., Bai, B., Wu, X. & Zhu, Z. A simple method for generating unidirectional surface plasmon polariton beams with arbitrary profiles. *Opt. Lett.* **40**, 5486 (2015).

Plasmons Generation

Experiment, SNOM data

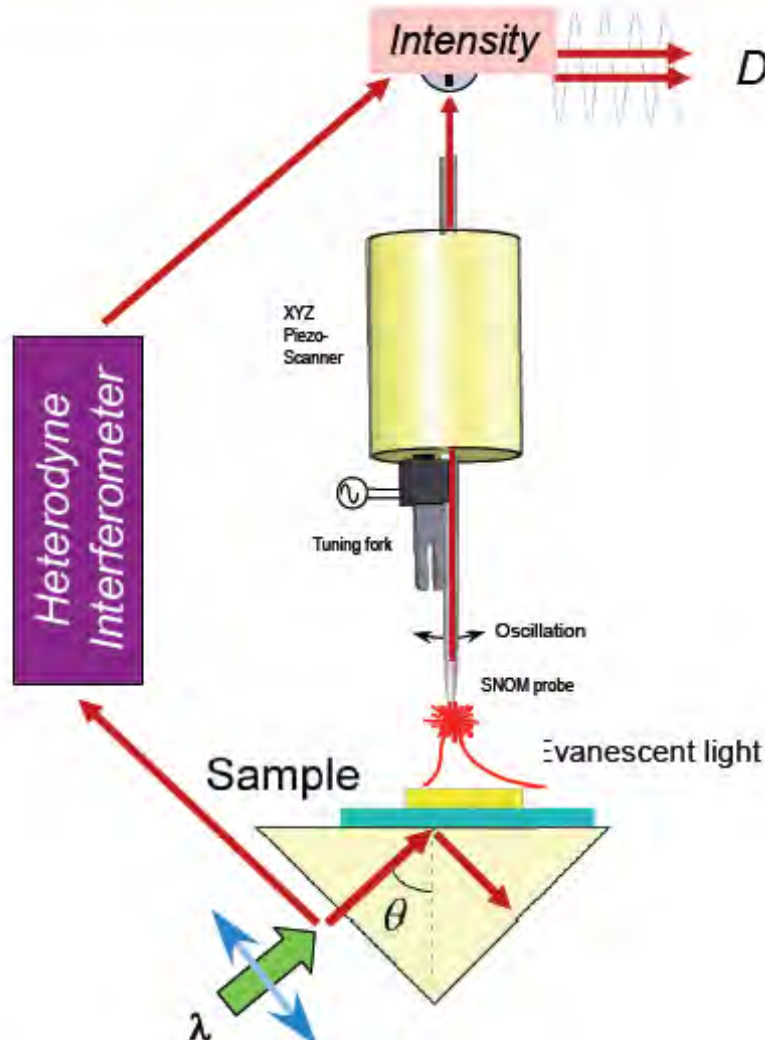


Simulation



Zhang, C. *et al.* Polarization-to-Phase Coupling at a Structured Surface for Plasmonic Structured Illumination Microscopy. *Laser Photonics Rev.* **12**, 1–7 (2018).

Amplitude and phase detection by SNOM



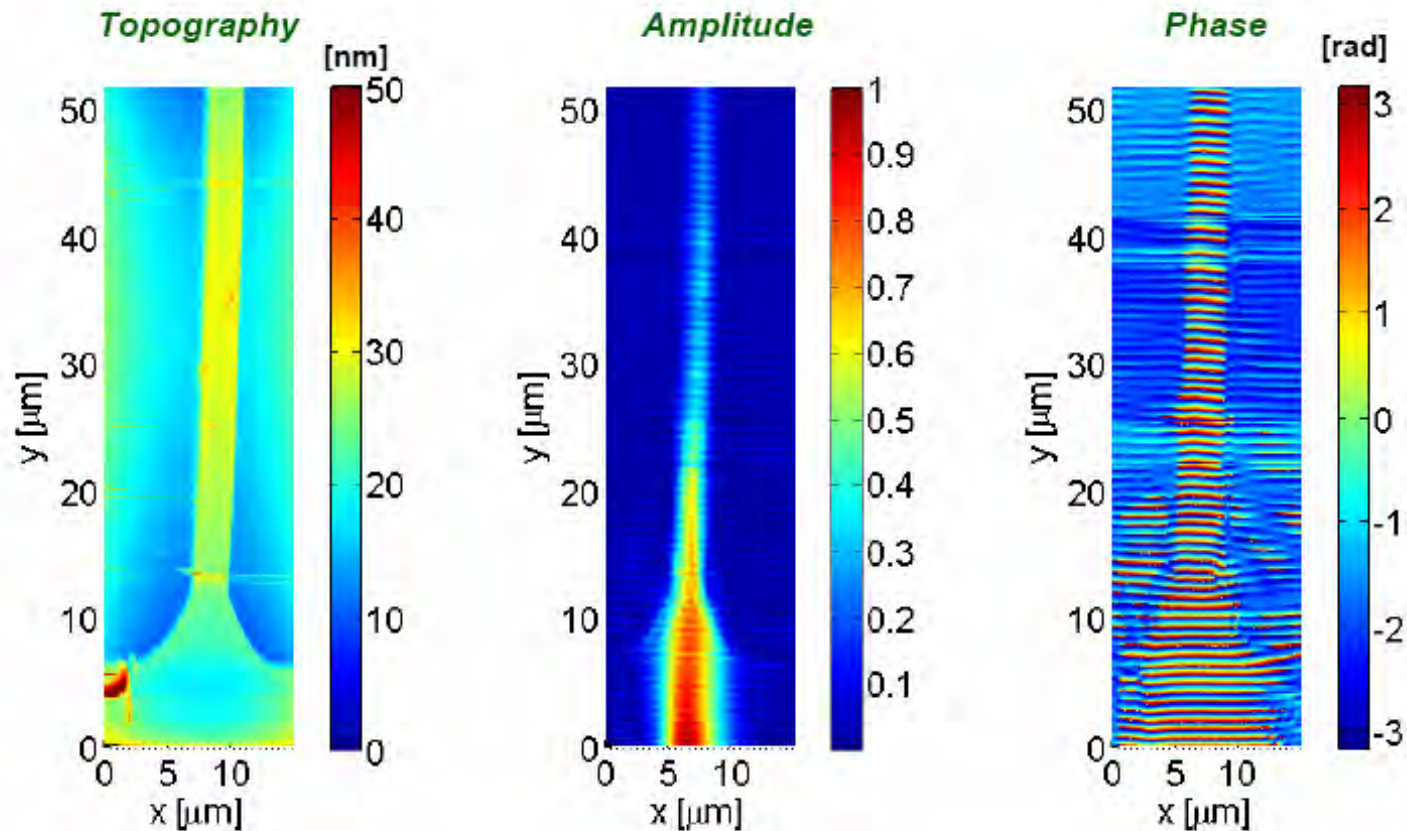
- PSTM = SNOM in collection mode
- Shear-force Atomic Force Microscope (AFM): topography.
- Usually Intensity recording only
- PSTM combined with a heterodyne interferometer) →

AMPLITUDE & PHASE

Plasmons on gold waveguide

3 μm wide WG

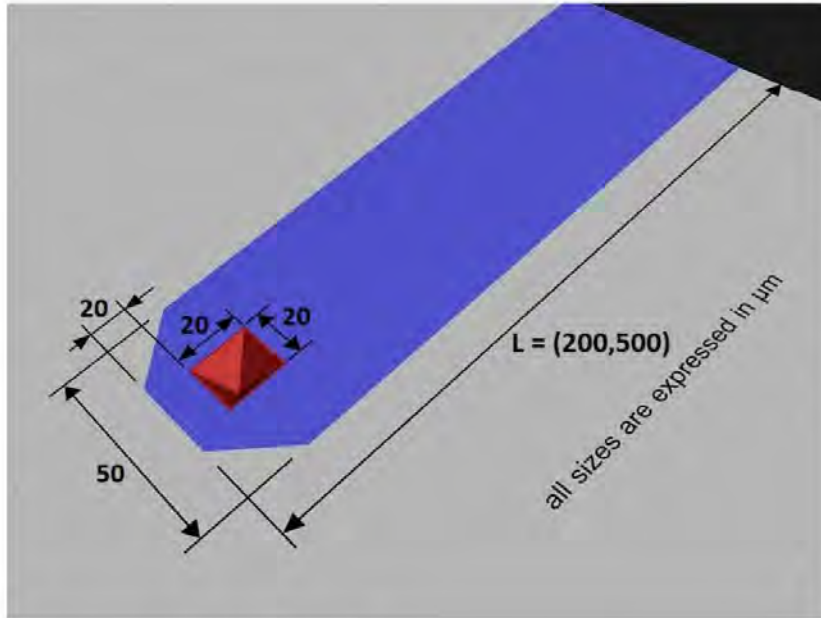
$\lambda = 785 \text{ nm}$



Antonello Nesci and Olivier J.F. Martin

cantilever SNOM: contact AND non-contact probes

1) Lever sizes and the pyramid position:

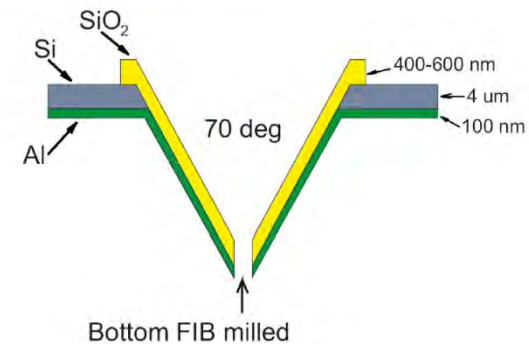


Pyramid LxWxH = 20x20x13 (70 deg)

	Spring Constant (N/m)			Frequency (kHz)			Length (micron)			Width (micron)			Thickness (micron)		
	Nominal	Min	Max	Nominal	Min	Max	Nominal	Min	Max	Nominal	Min	Max	Nominal	Min	Max
NonContact	16.5	5.9	39.0	130	88	180	200	190	210	55	54	57	4	3	5
Contact	1.01	0.41	2.30	20.8	15	27	500	490	510	55	54	57	4	3	5

Probe	Resolution	TR@ 473
1 contact	150 nm	$\sim 3 \cdot 10^{-4}$
1 contact	???	$0.3 \cdot 10^{-4}$
1 noncontact	110 nm	$\sim 0.16 \cdot 10^{-4}$
2 noncontact	120 nm	$\sim 0.5 \cdot 10^{-4}$
3 noncontact	135 nm	$\sim 0.7 \cdot 10^{-4}$
4 noncontact	100 nm	$\sim 0.2 \cdot 10^{-4}$
5 noncontact	150 nm	$\sim 1.6 \cdot 10^{-4}$

2) Tip shape and aperture size:



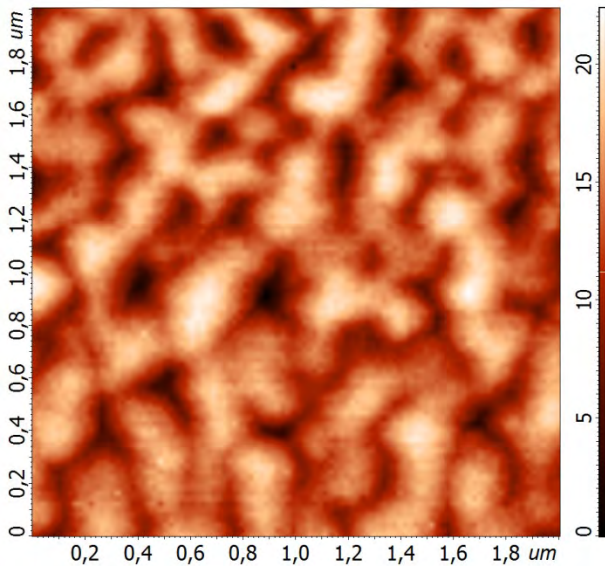
Pyramid (SiO₂) thickness 400-600 nm

3) Coating: Al, about 100 nm, coating from bottom side. Bottom FIB milling is done after coating. Typical aperture diameter about 170 ± 25 nm.

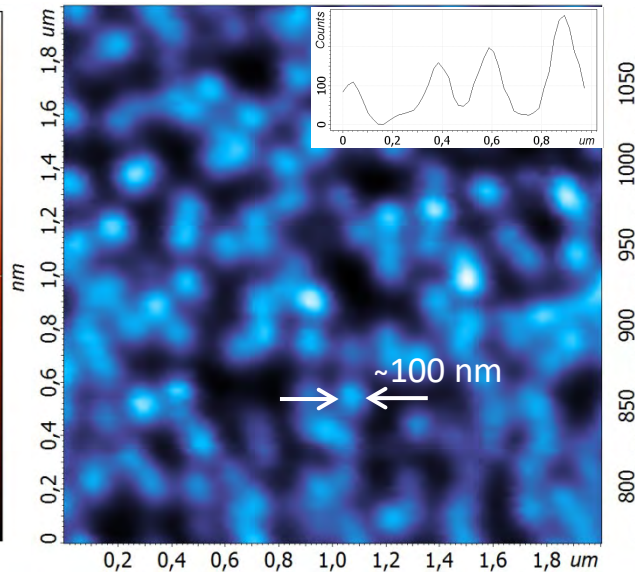


SNOM of InP/GaInP quantum dots with GaInP cap layer

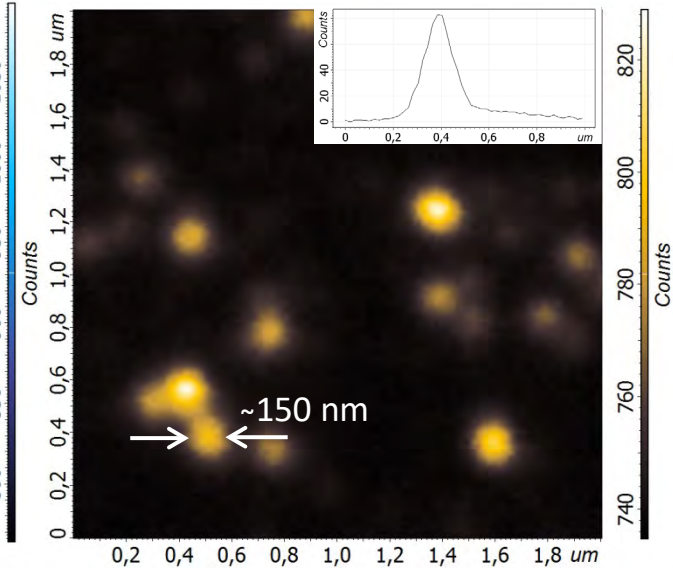
AFM Topography



PL SNOM, 700-770 nm



PL SNOM, 800-810 nm



Cap layer only (QDs not visible)

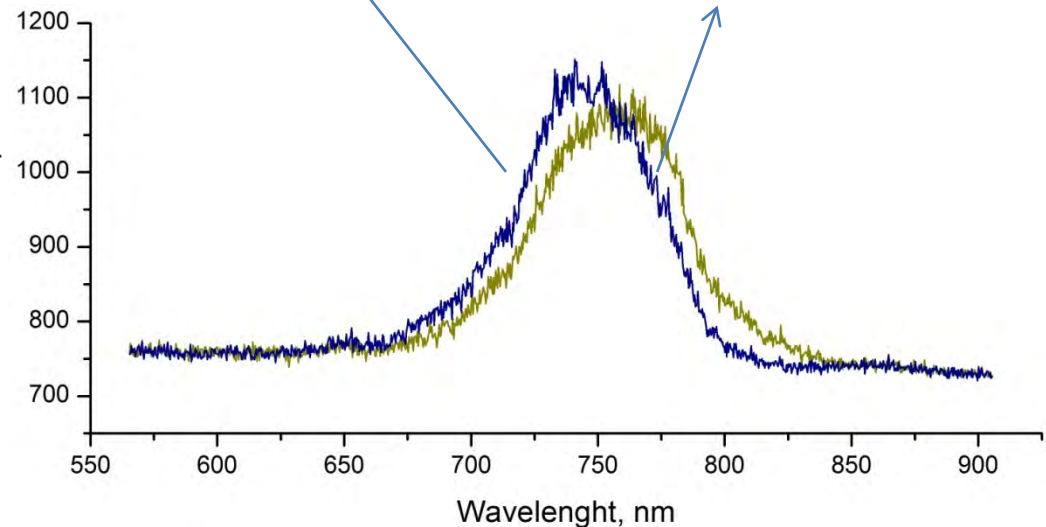
2x2 μm scans

20-50 nm dia. QDs

100-200 nm dia. QDs

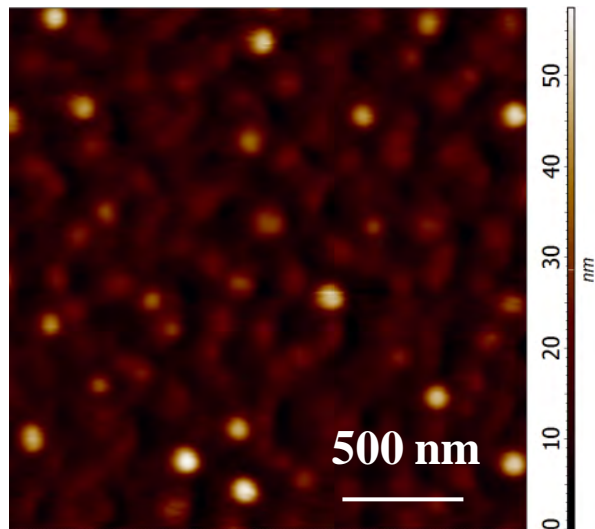
Simultaneously obtained topography (left) and SNOM maps of photoluminescence (PL) in 700-770 nm (center) and 800-810 nm (right) spectral regions. 100x100 pixels, 0.1 s/point

Images obtained by cantilever based SNOM in with excitation and collection via the same SNOM aperture

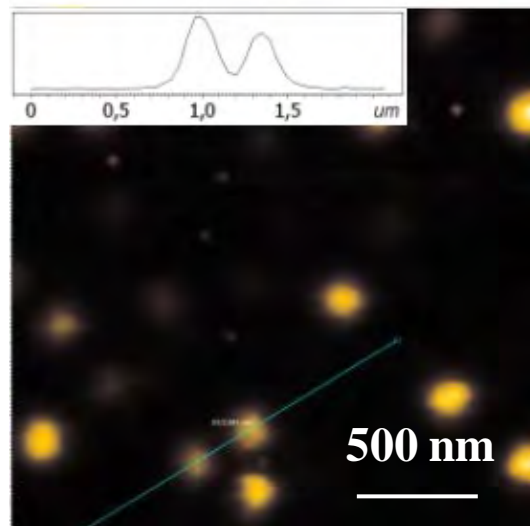


QD SNOM spectroscopy and topography

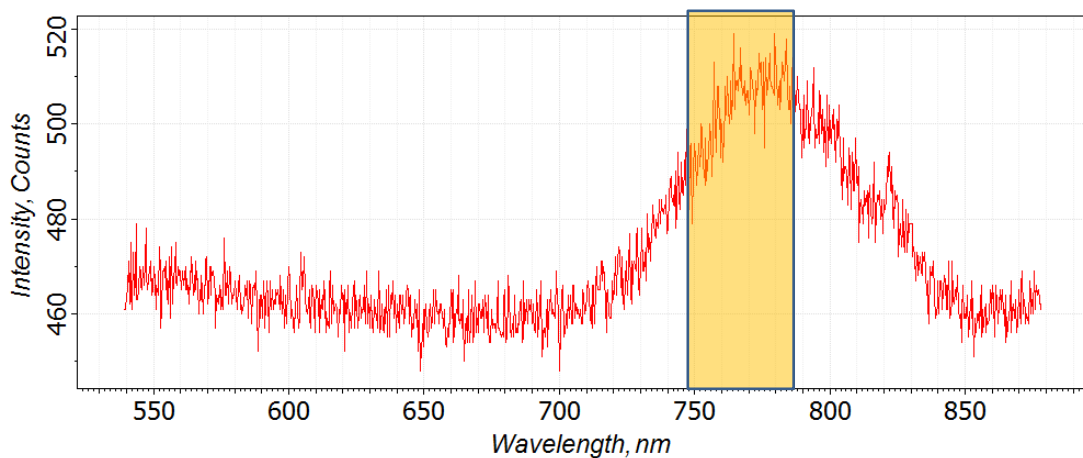
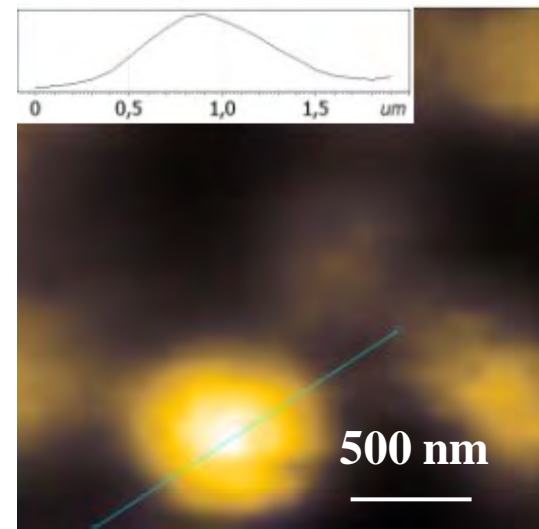
AFM Topography



SNOM PL, 750-780 nm



Confocal map, 750-780 nm



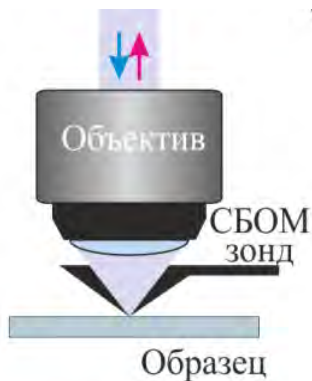
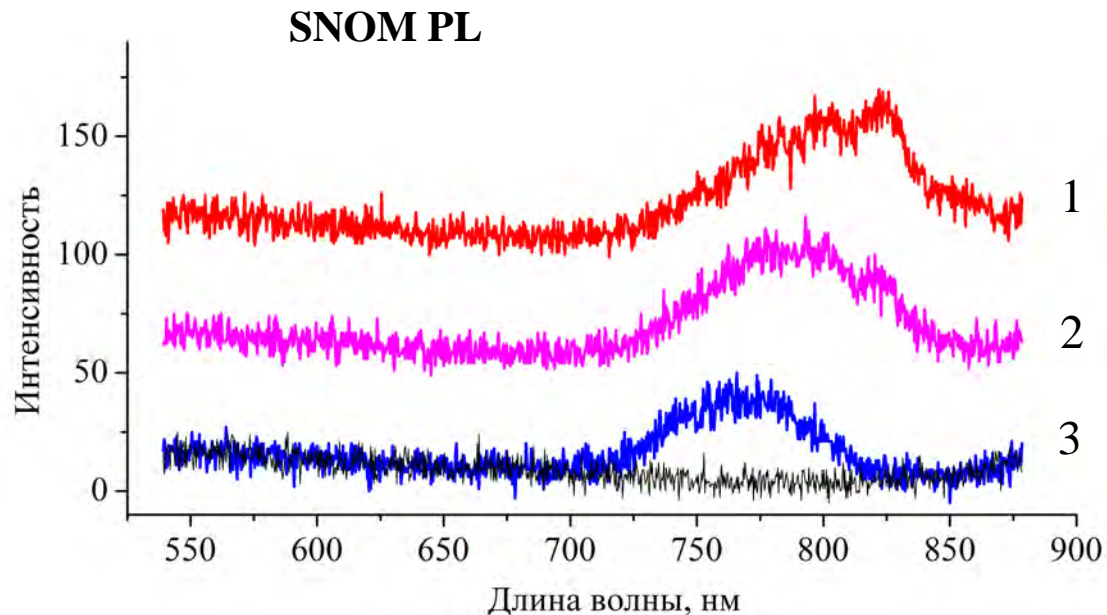
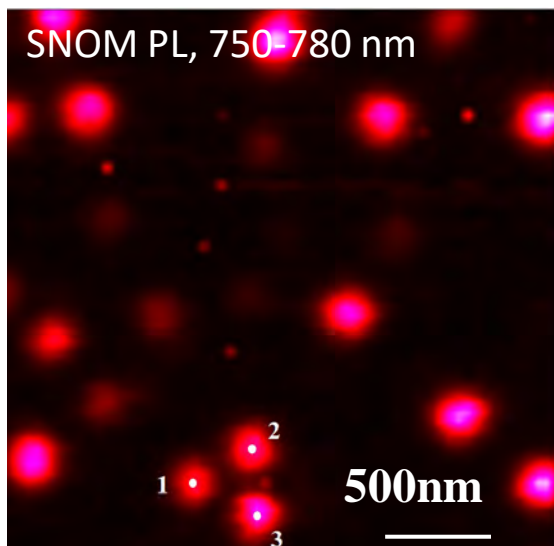
3x3 μm scans

Simultaneously obtained topography (left) and SNOM maps of photoluminescence (PL) in 750-780 nm band (center) and confocal map with the same spectral band (right). 100x100 pixels, 0.1 s/point. Images obtained by cantilever based SNOM in with excitation and collection via the same SNOM aperture. AFM tapping mode used.

Shelaev A. V., Mintairov A. M., Dorozhkin P. S., and Bykov V. A. Scanning near-field microscopy of microdisk resonator with InP/GaN quantum dots using cantilever-based probes // J. Phys. Conf. Ser. 2016. Vol. 741. P. 12132.

Single QD SNOM spectroscopy

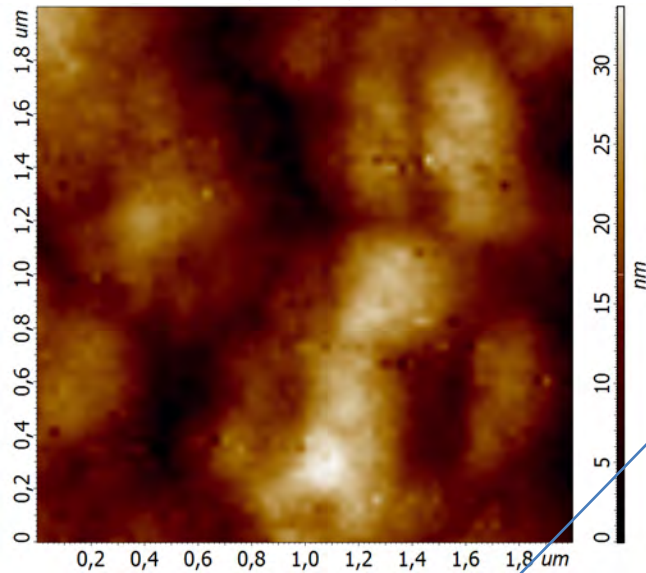
InP/GaInP quantum dots with no cover layer



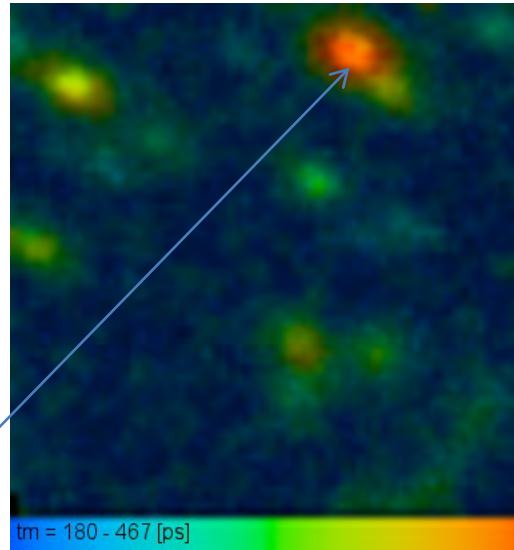
Thanks to high transmission of cantilever-based SNOM probes and high system sensitivity it is possible to detect single point spectrum with exposure time of few seconds per point. And distinguish spectra from single quantum dots which are less than 500 nm away from each other. Clear difference in PL spectra is observed.

Fluorescence lifetime (FLIM) SNOM microscopy of InP/GaInP quantum dots

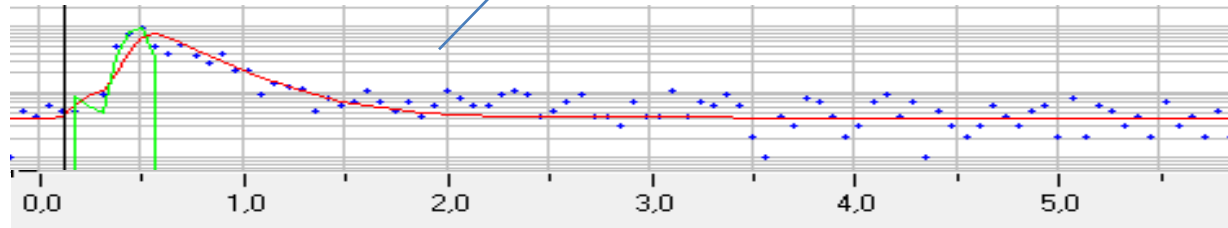
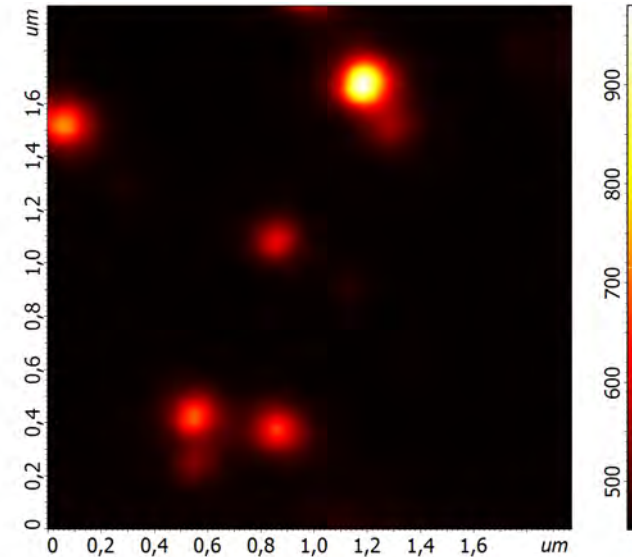
AFM Topography



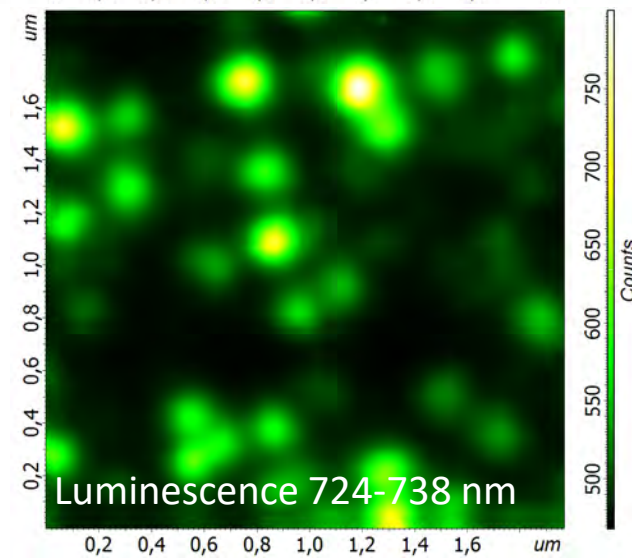
Lifetime map 750-770 nm



Luminescence 780-800 nm

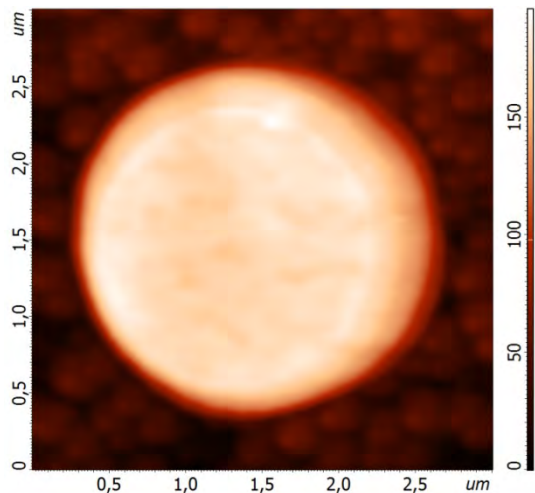


Topography (left) and FLIM mapping of 750-770 nm band (center) and luminescence intensity 780-800 nm (right up) and 724-738 nm (right bottom). Decay curve on the bottom left image.

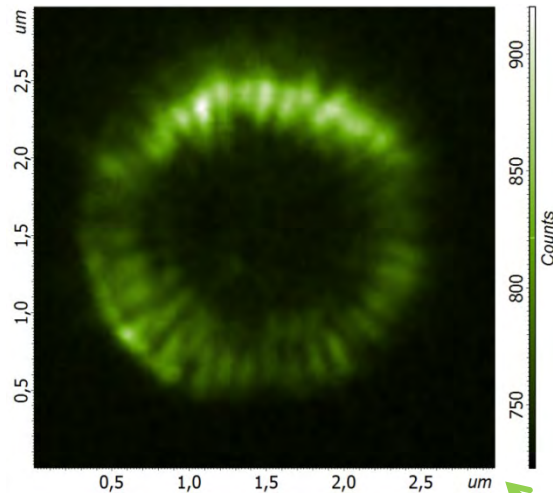


Whispering gallery light modes in microdisks with InP/GaInP self-organized quantum dots

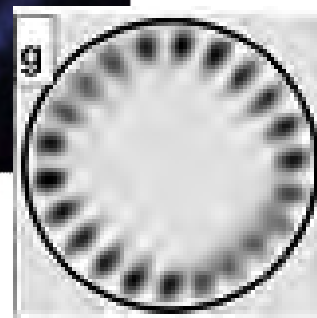
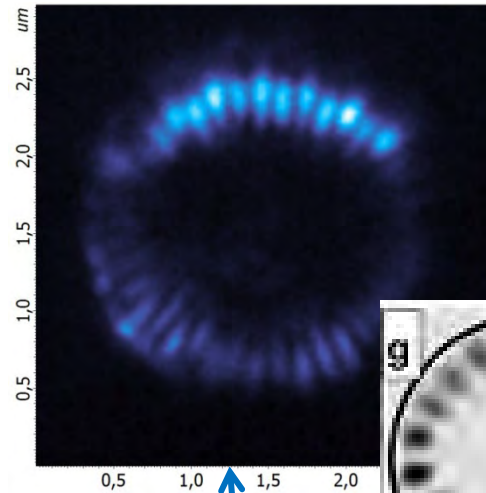
Topography



SNOM PL, 732-735 nm
TE₂₀ mode

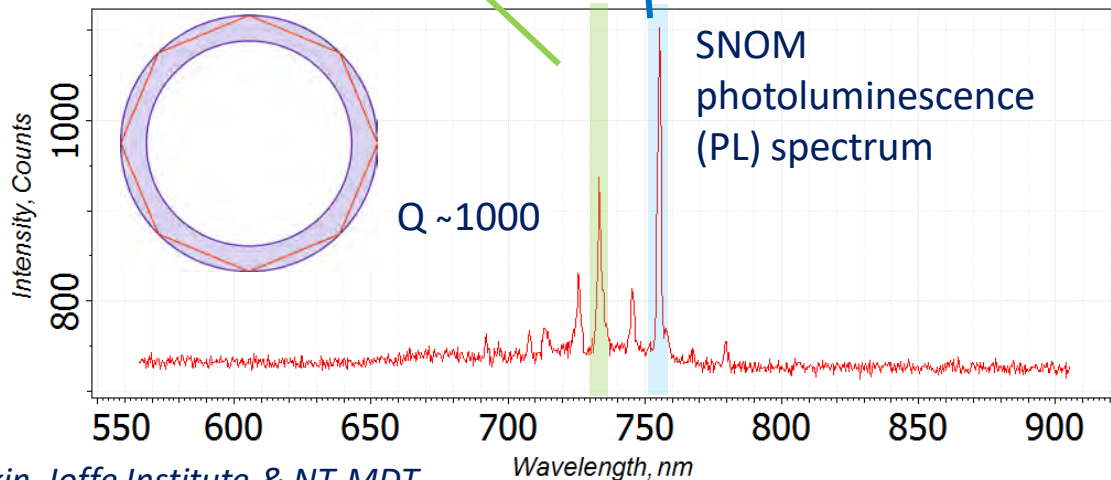


SNOM PL, 753-757 nm
TE₁₈ mode



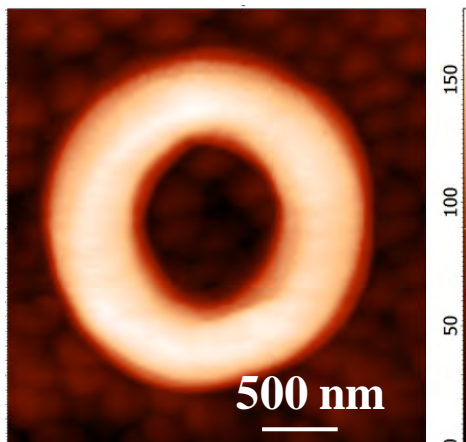
Simultaneously obtained topography (left) and SNOM maps of light whispering gallery modes in the ranges 753-757 nm band (center) and 732-735 nm (right). 100x100 pixels, 0.1 s/point

Images obtained by cantilever SNOM with side illumination

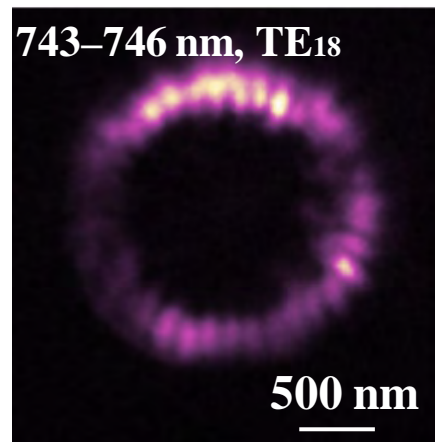


Whispering gallery light modes in microrings with InP/GaInP self-organized quantum dots

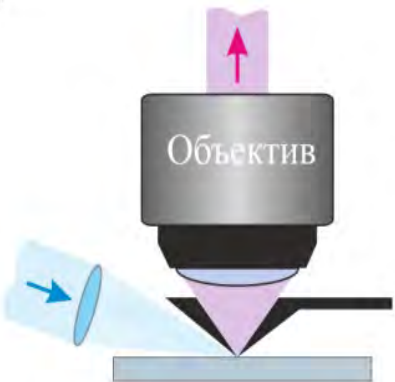
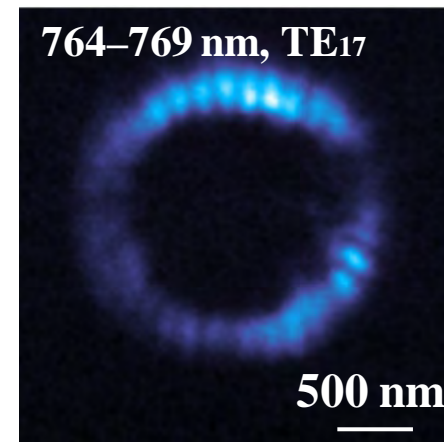
AFM topography



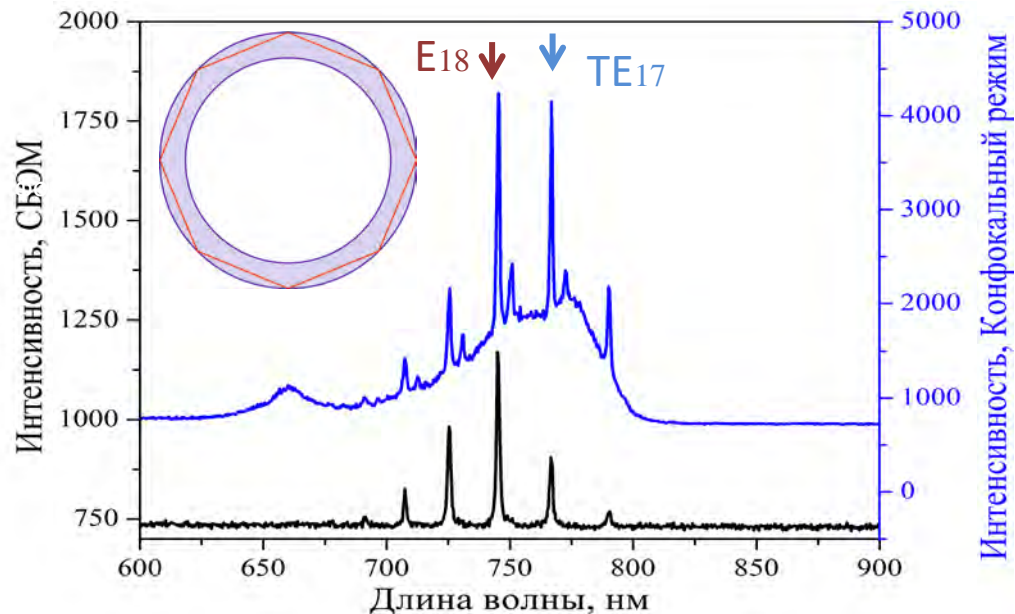
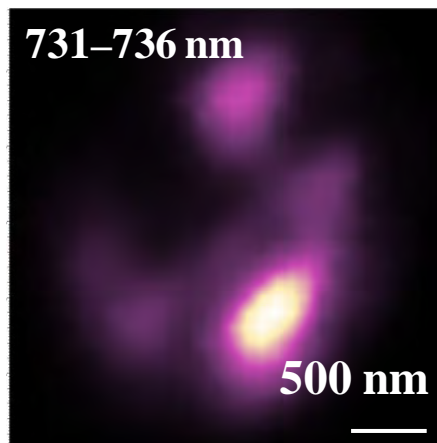
SNOM



SNOM



Confocal mode



Shelaev A. V., Mintairov A. M., Dorozhkin P. S., and Bykov V. A. Scanning near-field microscopy of microdisk resonator with InP/GaInP quantum dots using cantilever-based probes // J. Phys. Conf. Ser. 2016. Vol. 741. P. 12132.

Laser emission in 3D studied by SNOM

Calculation (XZ section)



Experiment (XZ section)



Experiment (XY section)

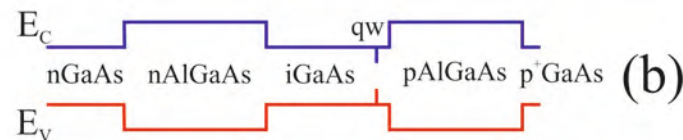
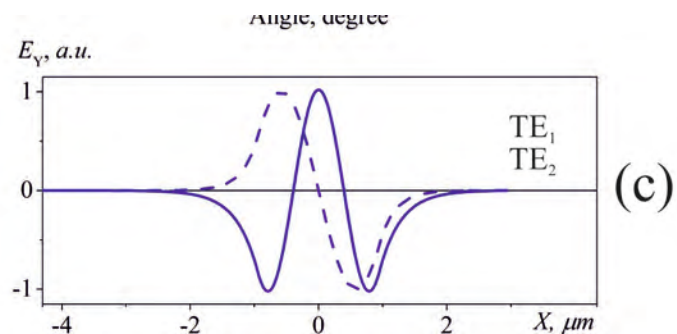


Cantilever SNOM operation at near IR region ($\sim 1.1 \mu\text{m}$)

← Far field (propagating e-m radiation)

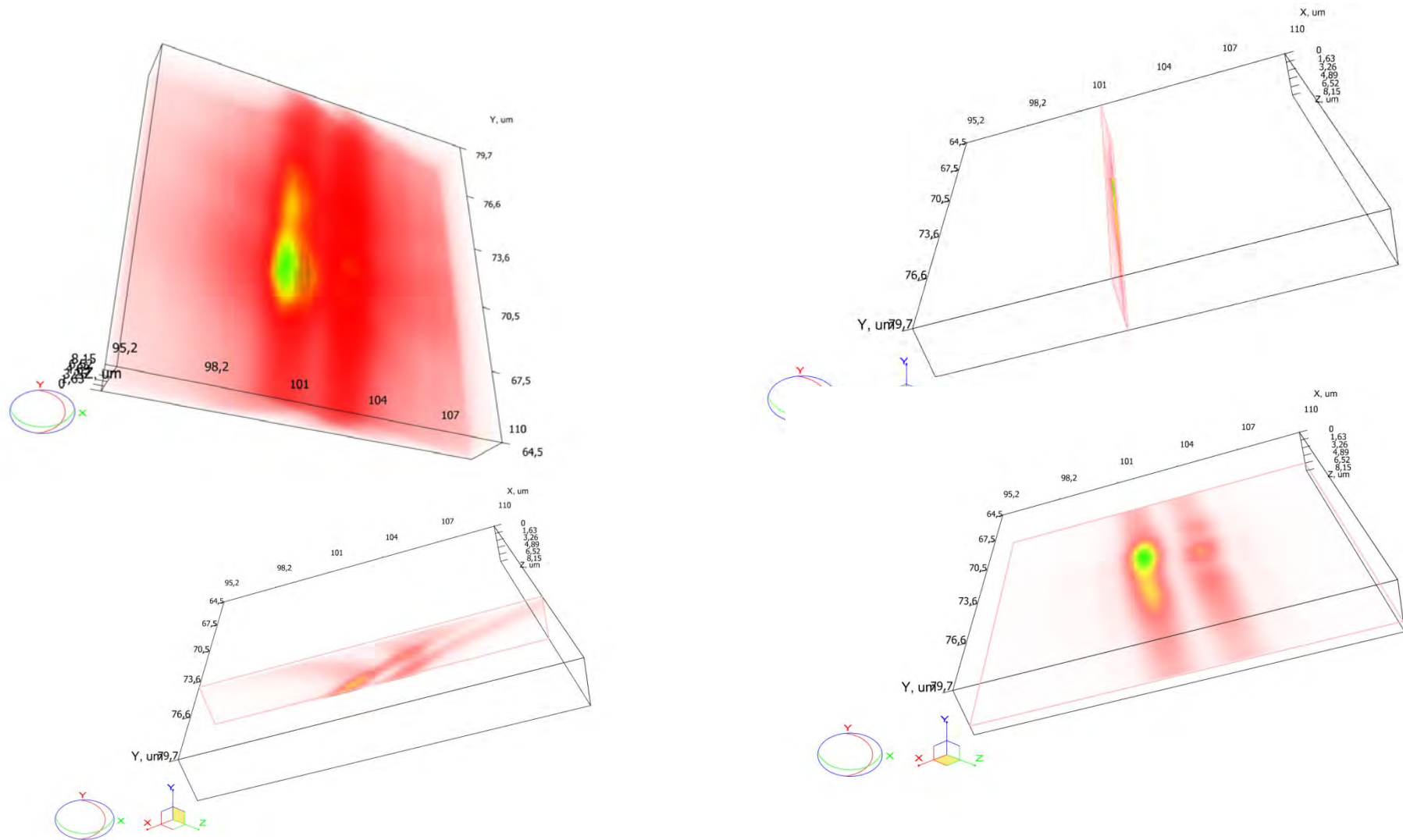
← Surface (near field)

← Surface (near field)



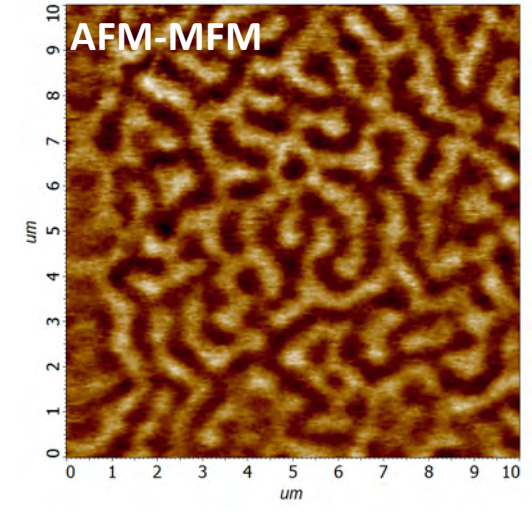
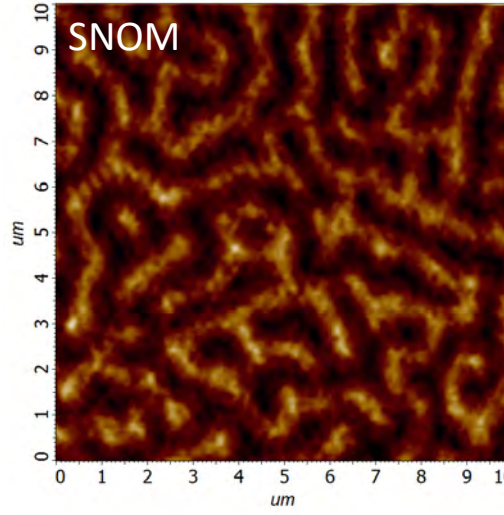
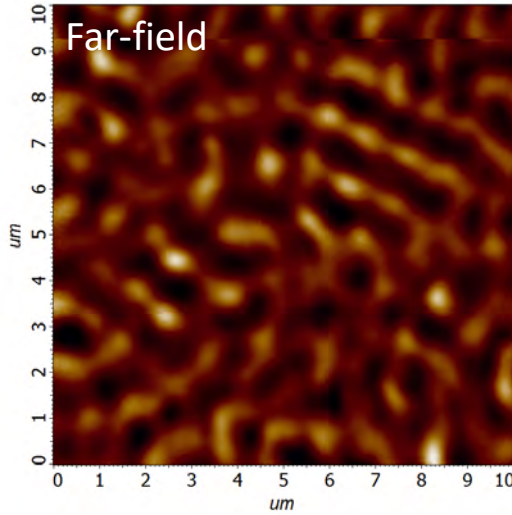
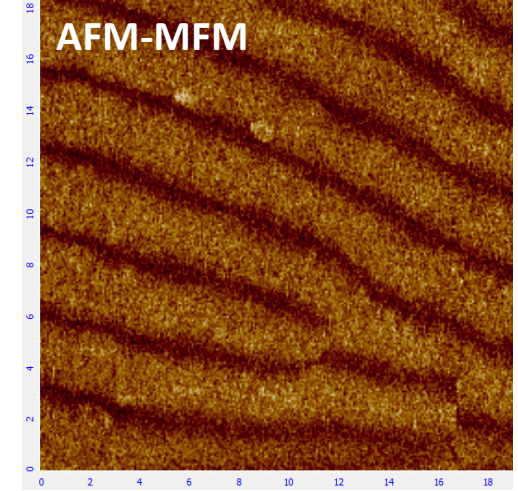
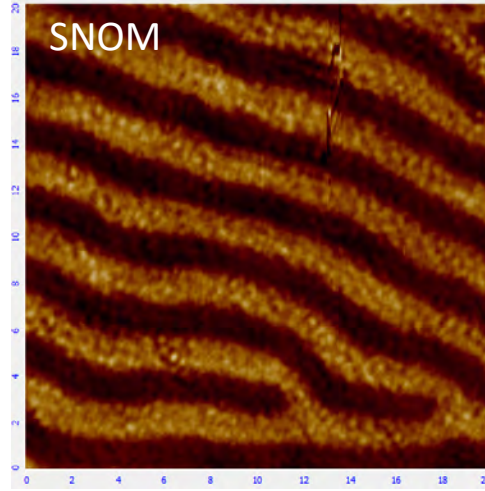
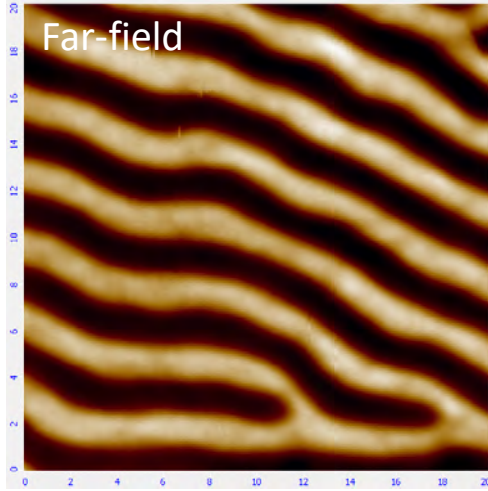
A.V. Ankudinov, P.S. Dorozhkin, A.A. Podoskin, A.V. Shelaev, S.O. Slipchenko, I.S. Tarasov, M.L. Yanul
Ioffe Physical Institute; NT-MDT Co. & ITMO

Laser emission in 3D studied by SNOM



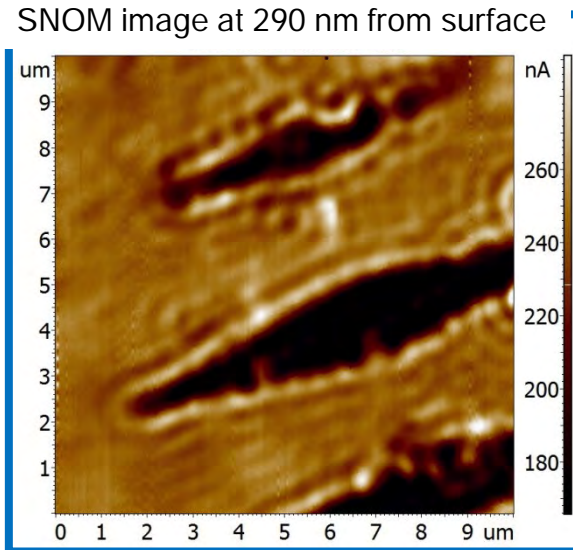
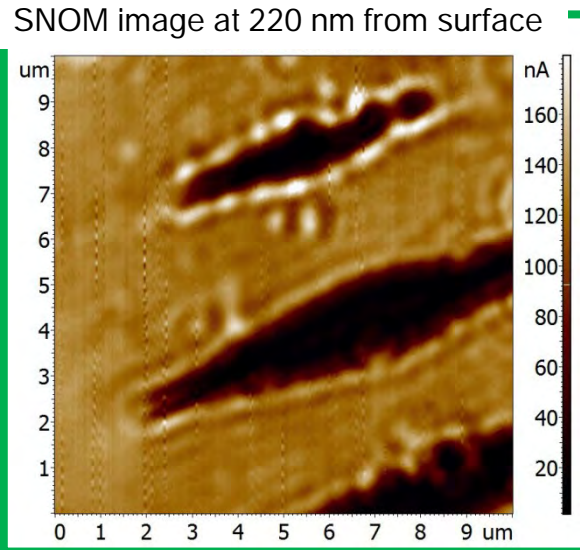
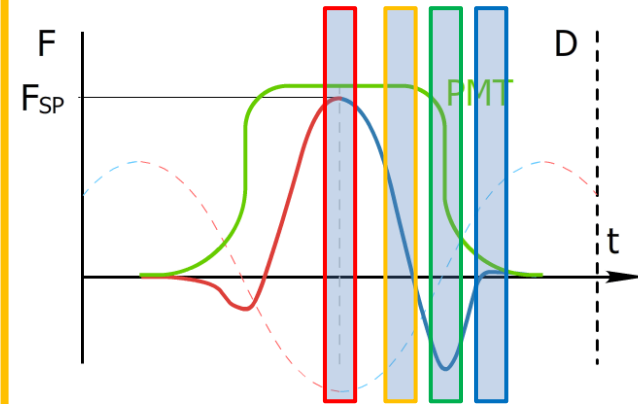
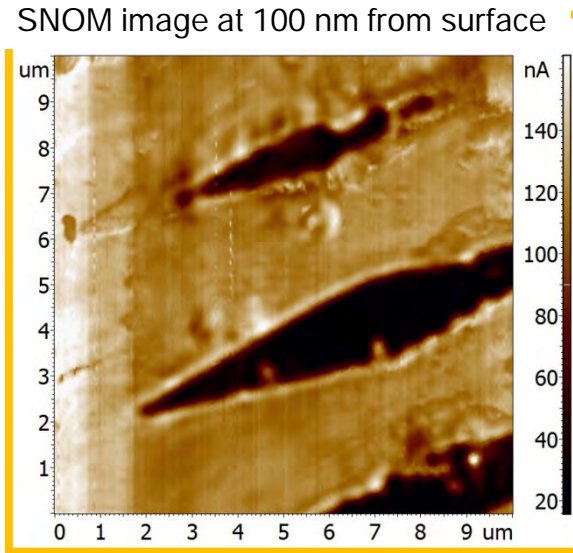
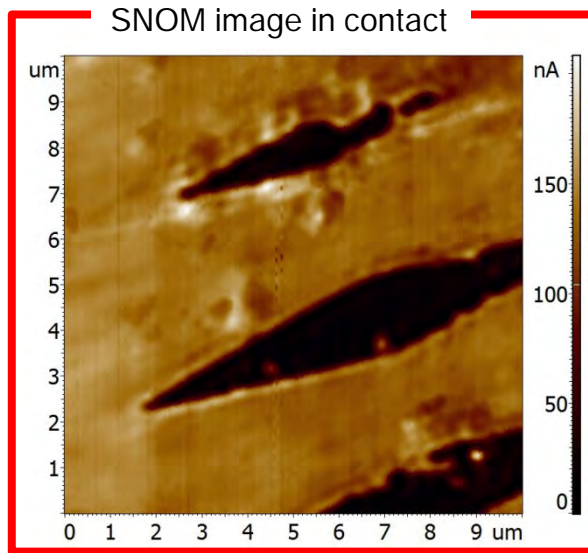
3D emission intensity distribution
XY, XZ and YZ cross-sections

Magneto-optic effects investigation by SNOM: thin film of YIG



Far-field and near-field cross-polarization images from the same area of thin garnet film 20x20 μm (top) and 10x10 μm (bottom). 473 nm laser used. Comparison with MFM images from same sample (right).

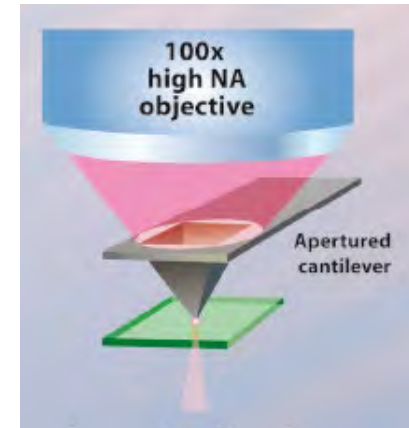
SNOM in Hybrid regime



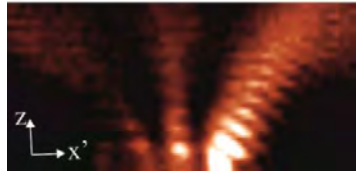
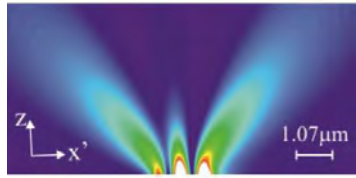
SNOM images (obtained in HD mode). SNOM images were done simultaneously, in HD mode, by choosing different boundaries for averaging of the signal. The images were done in HD mode on SNG01 grating.

Key features of cantilever SNOM

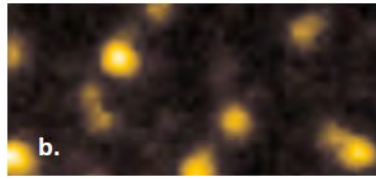
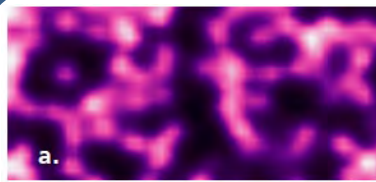
- ✓ High mechanical durability of the probes
- ✓ Stability under strong laser illumination (up to 30 mW in a focused spot)
- ✓ Very high resolution (NA) objectives used to focus/collect light onto/from SNOM aperture (1.0 NA, 280 nm resolution in liquid; 0.7 NA 400 nm resolution in air)
- ✓ Precise and reproducible automated positioning of the laser spot on SNOM cantilever aperture (positioning precision and stability <5 nm)
- ✓ Non-contact SNOM cantilevers (allows lock-in detection of SNOM signal; allows advanced AFM modes, e.g. KFM *simultaneously* with SNOM imaging)
- ✓ Measurements in liquid
- ✓ Measurements with heating up to 150 C



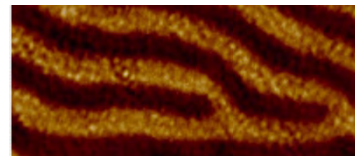
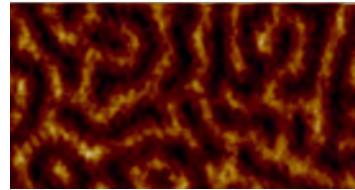
Aperture SNOM applications



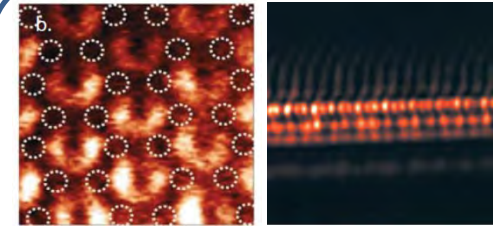
Lasers



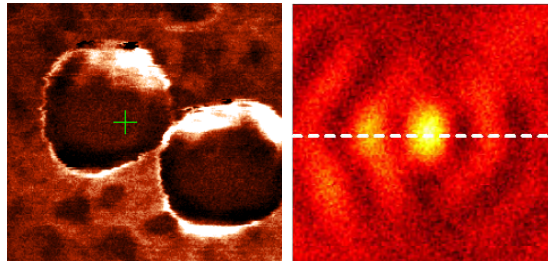
Quantum dots



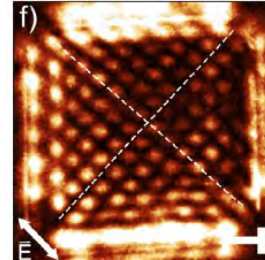
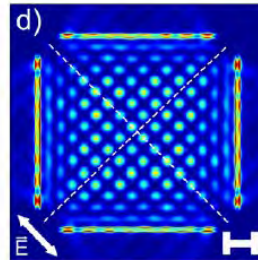
Magnetic domains



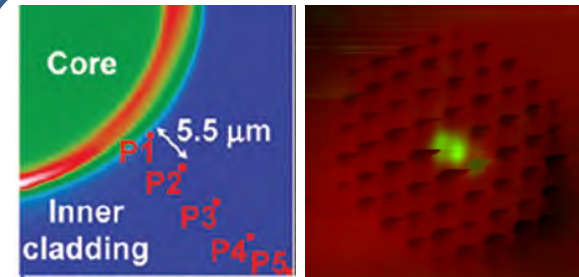
Photonic crystals



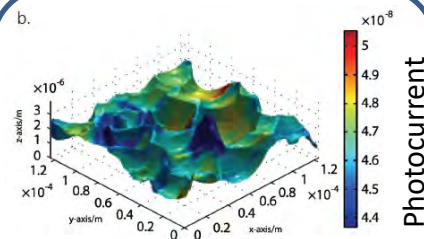
E - m field in plasmonic structures



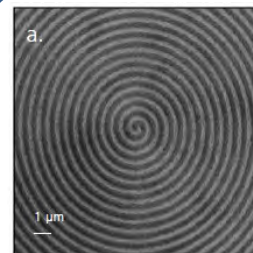
Surface plasmon polaritons



Optical fibers

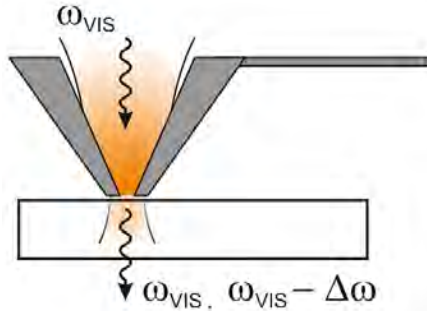


Photovoltaics



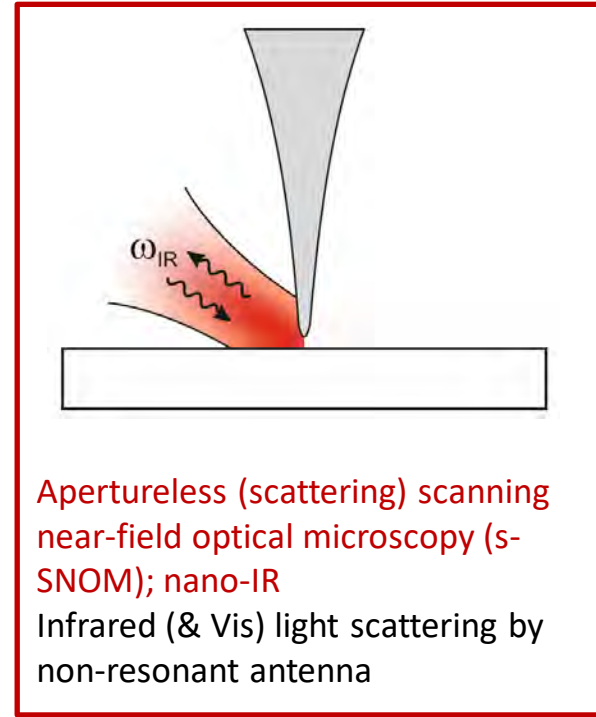
Optical micro-devices

Super-resolution imaging using scanning optical antennas



Aperture scanning near-field optical microscopy (SNOM)

Light transmission through non-resonant subwavelength aperture

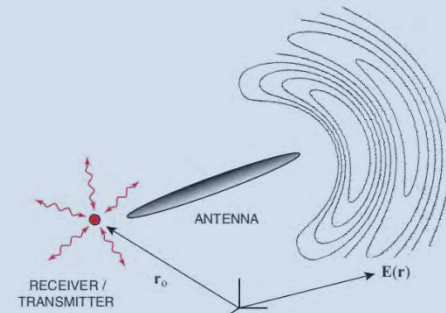


Apertureless (scattering) scanning near-field optical microscopy (s-SNOM); nano-IR

Infrared (& Vis) light scattering by non-resonant antenna

Optical antenna: a device designed to efficiently convert free-propagating optical radiation to localized energy, and vice versa.

- L. Novotny, N. van Hulst, *Nature photonics* 5, 89 (2011)
- P. Bharadwaj, B. Deutch, L. Novotny, *Adv. In Opt. Phot.* 1, 438 (2009)
- Pohl D. W., *Optics, Principles and Applications* (World Scientific, 2000).



Scattering (apertureless) SNOM: mapping sample dielectric permittivity $\epsilon(\omega)$ under light illumination

Light scattered by “tip+sample” configuration:

$$E_{sc} \propto \alpha_{eff}(\epsilon_s, z_{ts}) \cdot E_{loc}$$

$\epsilon_s(\omega)$ - dielectric permittivity of sample

z_{ts} - tip-sample distance

E_{loc} - excitation light field

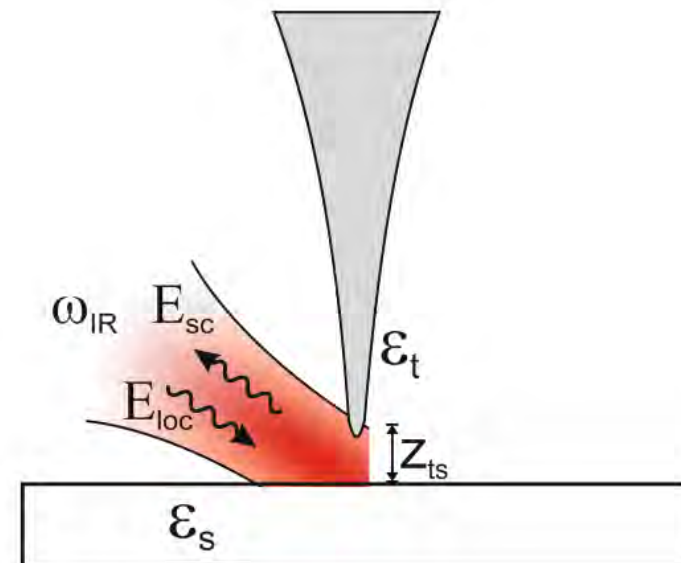
E_{sc} - scattered light field

α_{eff} - effective polarizability of “tip+sample” configuration

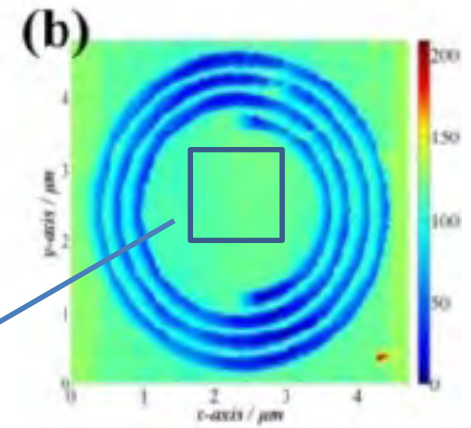
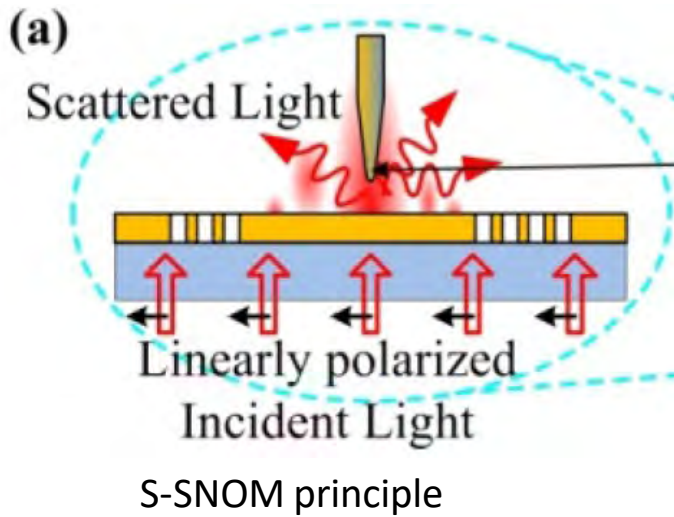
$$\alpha_{eff} = \frac{\alpha(1-\beta)}{1 - \frac{\alpha\beta}{32\pi(z+a)^3}}$$

$$\alpha = 4\pi a^3 \frac{\epsilon_t - \epsilon_i}{\epsilon_t + 2\epsilon_i} \text{ and } \beta = \frac{\epsilon_s - 1}{\epsilon_s + 1}$$

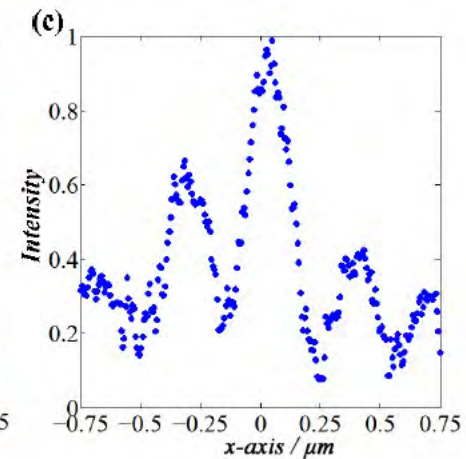
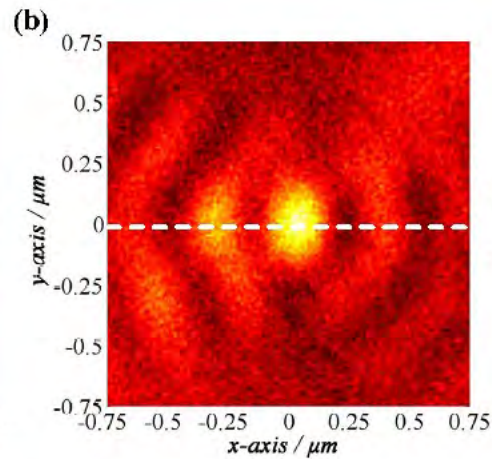
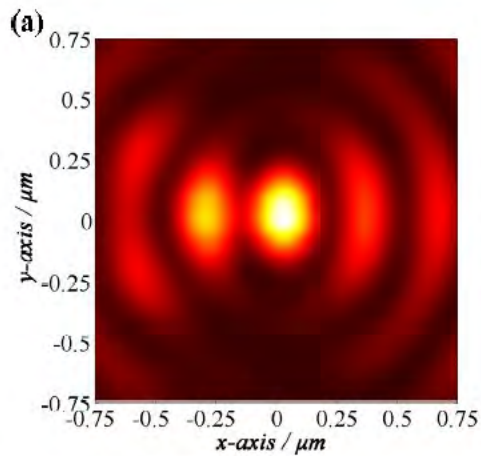
$\epsilon_t(\omega)$ - dielectric permittivity of tip



sSNOM to study localized electromagnetic field



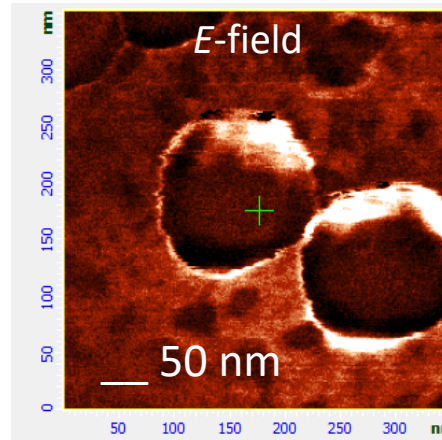
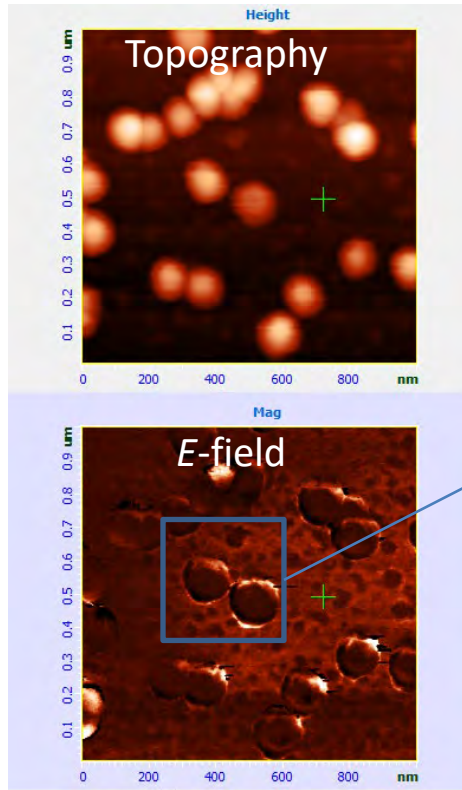
Plasmonic lens (AFM image)



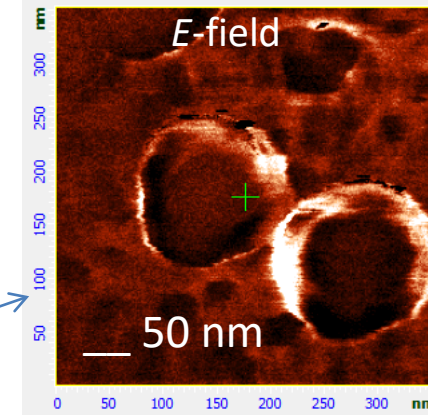
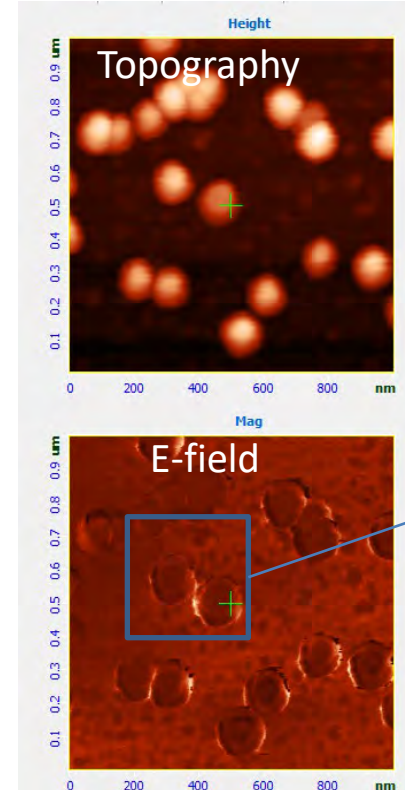
Calculated (a) and measured (b,c) longitudinal E -field component of light on the surface of a plasmonic lens

EM field visualization by sSNOM

Data courtesy: Andrey Aristov, and Andrei Kabashin
Aix Marseille University, CNRS, Marseille, France



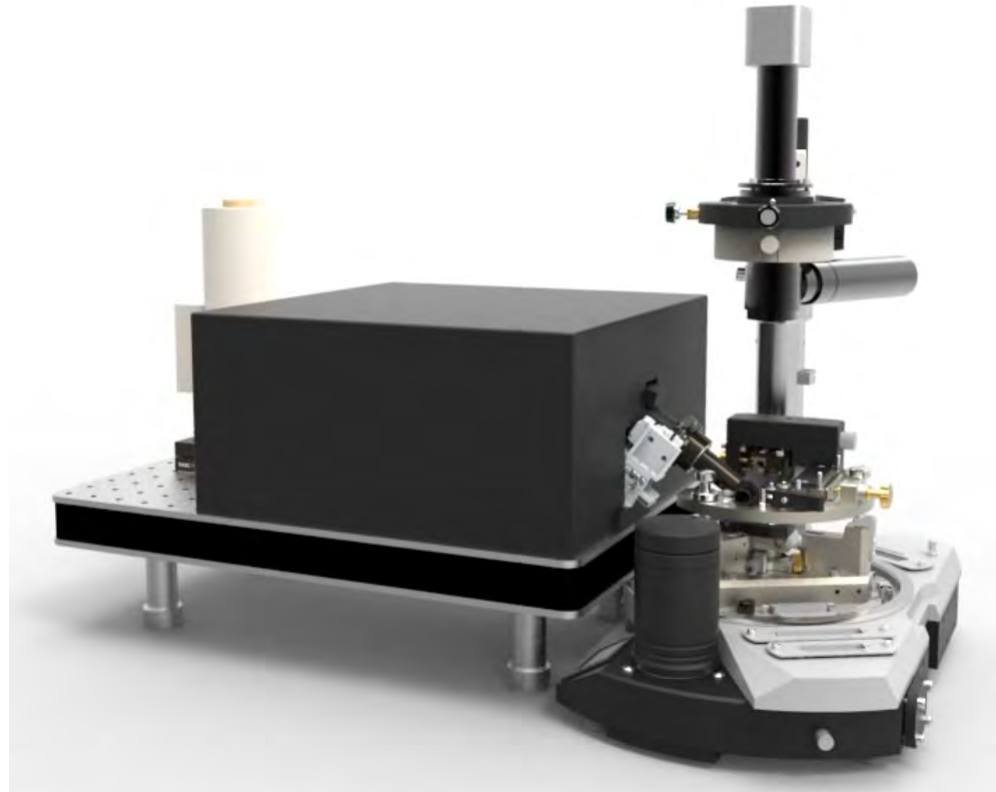
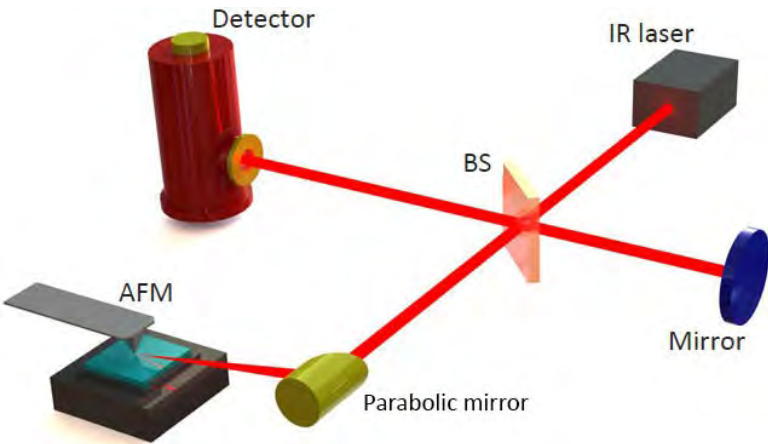
↑ Vertical polarization



→ Horizontal polarization

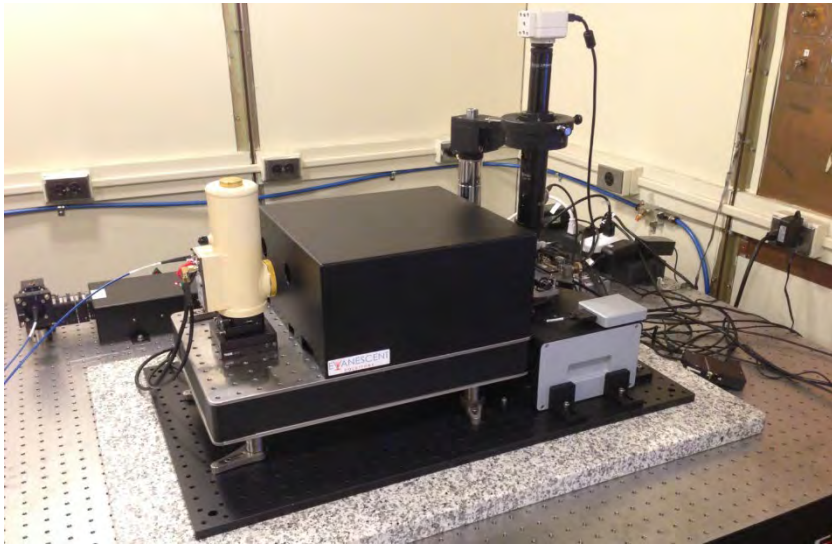
Direct visualization of localized electromagnetic field in Au nanoparticles (SERS substrate). 633 nm

NTEGRA Nano IR

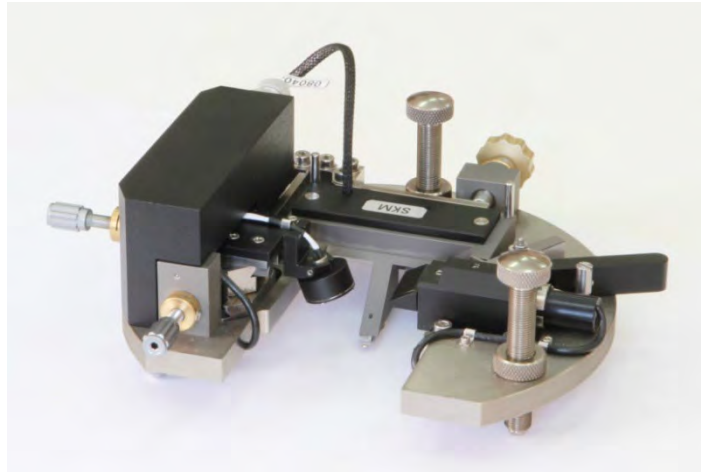


- IR microscopy and spectroscopy with 10 nm resolution
- Wide spectral range of operation: 3-12 μm
- Incredibly low thermal drift and high signal stability
- Versatile AFM with advanced modes: SRI (conductivity), KPFM (surface potential), SCM (capacitance), MFM (magnetic properties), PFM (piezoelectric forces)
- Hybrid Mode™ - quantitative nanomechanical mapping

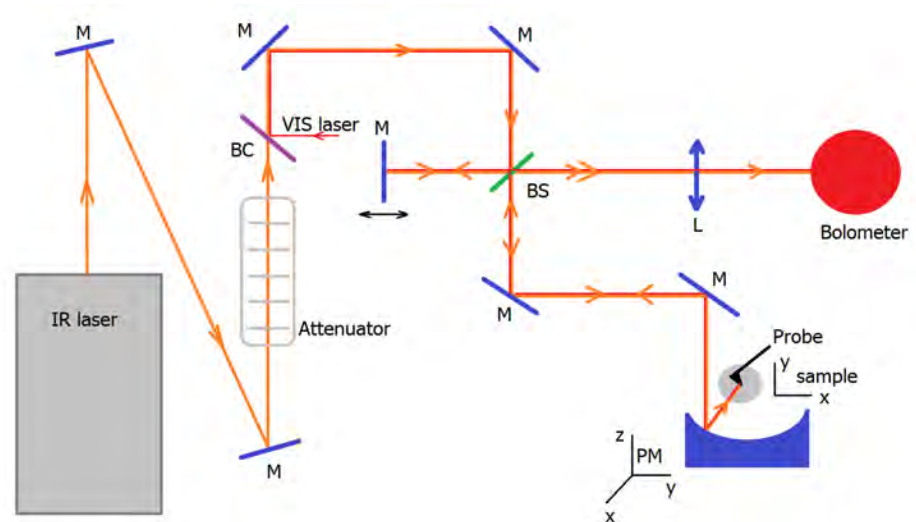
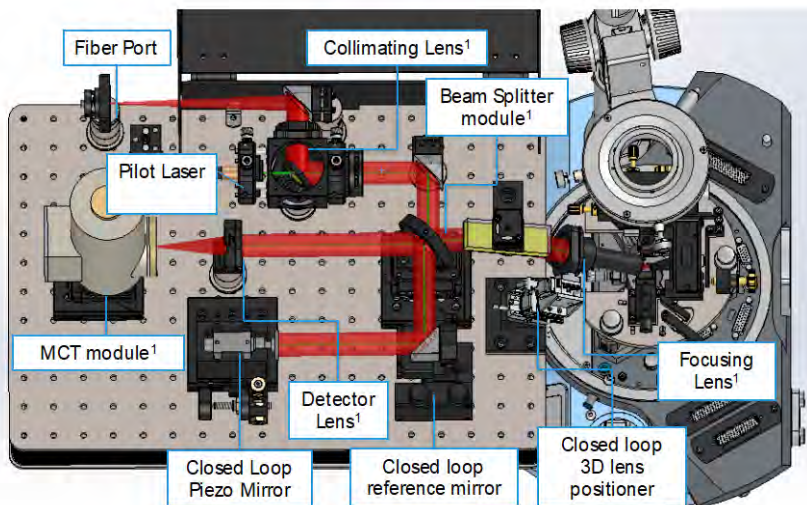
NTEGRA Nano IR



NTEGRA Nano IR, Stony Brook Univ., NY, USA

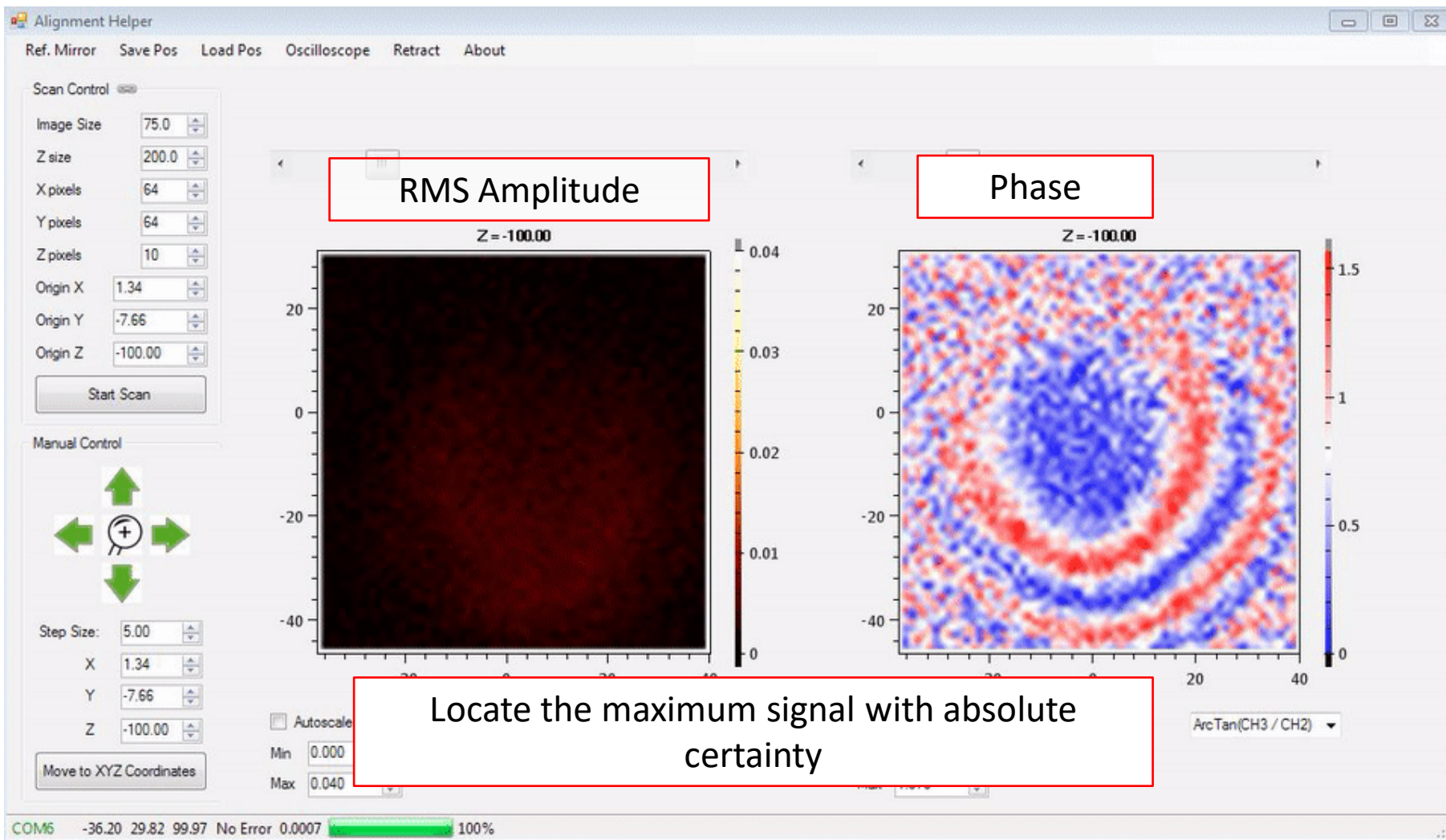


Measuring head



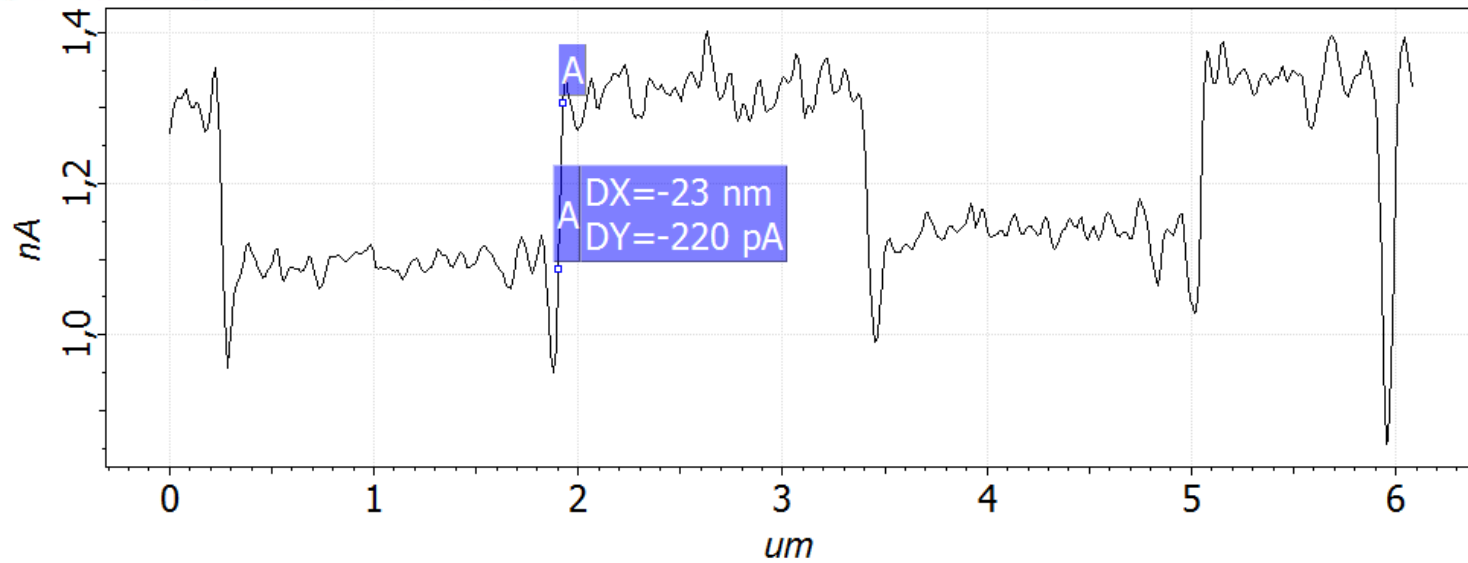
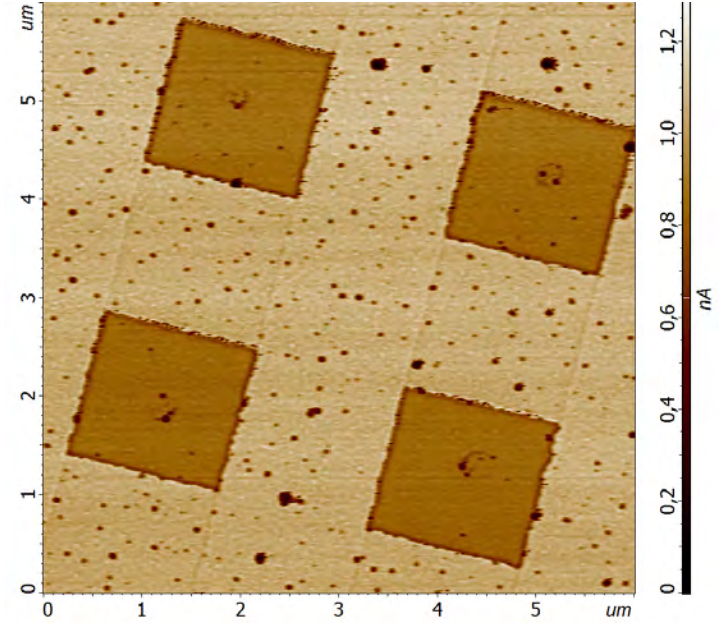
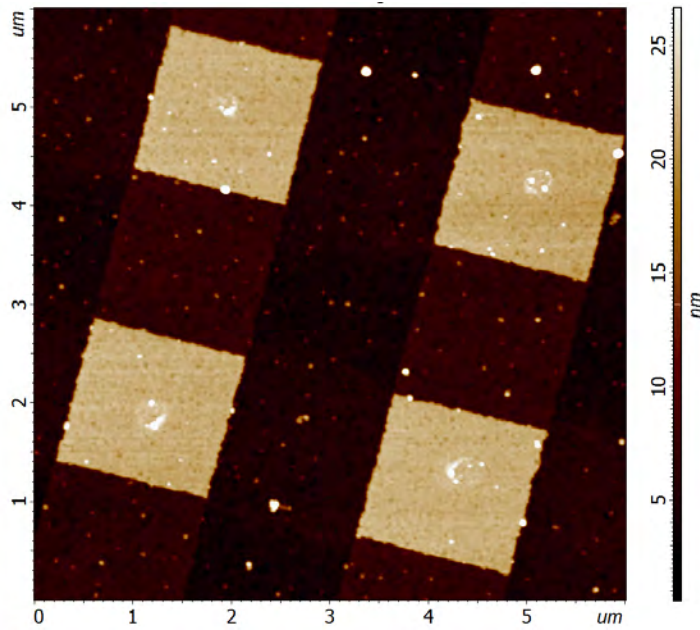
Optical schemes

Demonstration of hot-spot alignment, 10 scans over 200um of focus adjustment



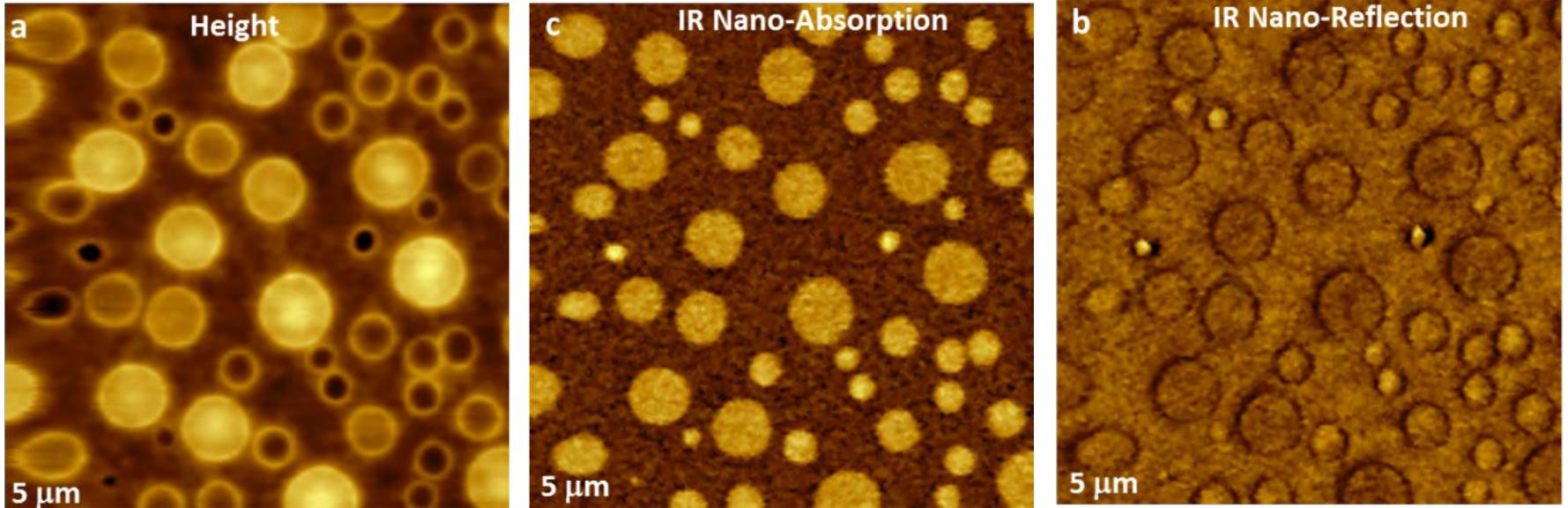


NTEGRA Nano IR: TGQ Si/SiO₂ grating



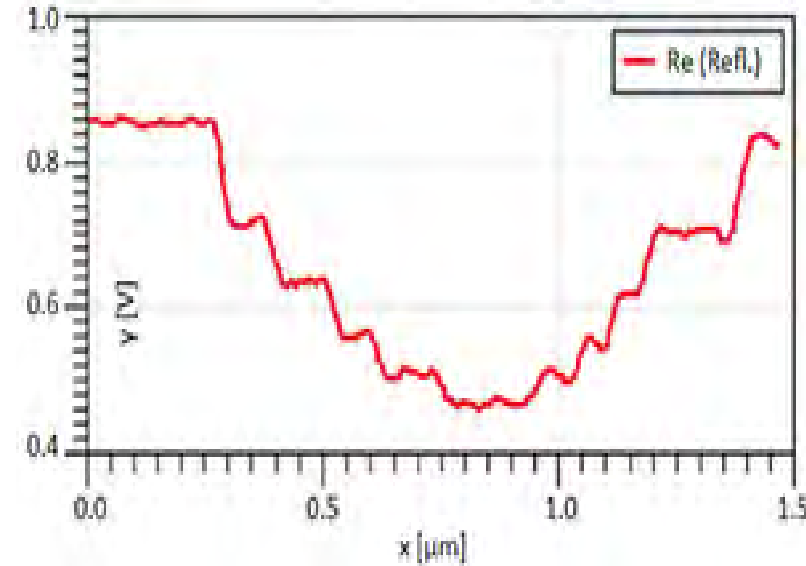
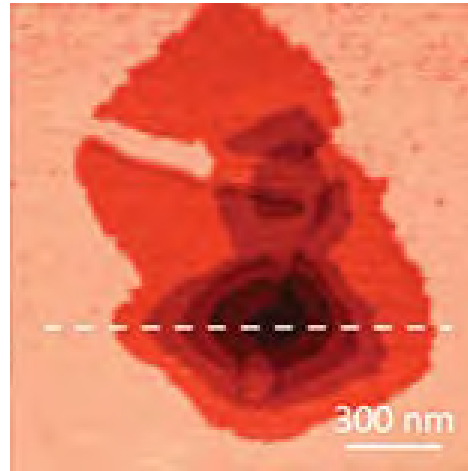
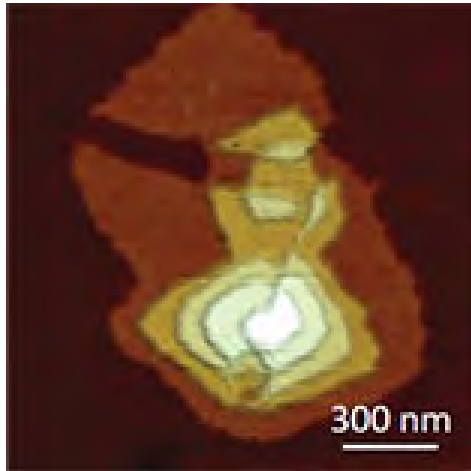
Cross section of the optical near-field Amplitude

NTEGRA nano IR: PS/PVAC blend on ITO



Height (a), nano-reflection ($\lambda = 10.6 \text{ mm}$), (b) and nano-absorption ($\lambda = 10.6 \text{ mm}$) (c) images of a PS/PVAC film on ITO substrate.

NTEGRA IR: oligothiophene monolayers on Si

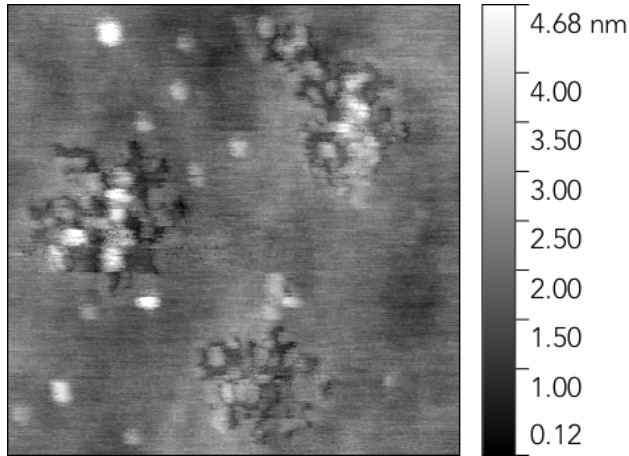


IR reflection contrast of thin and soft structures easily detectable. Each of five 3.4 nm steps is resolved. Spatial resolution is better than $\lambda/1000$.

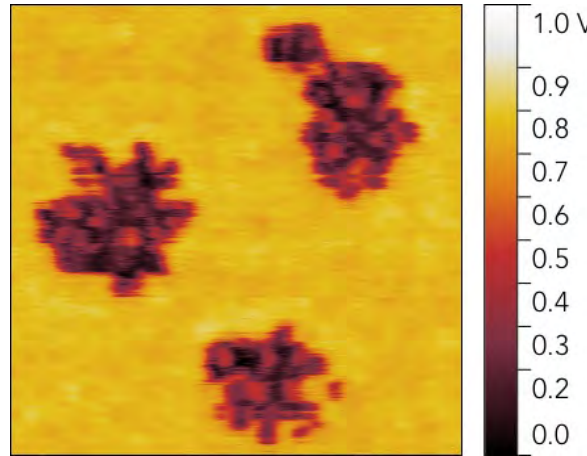
Sample courtesy to Dr. A. Mourran (DWI, Aachen, Germany). Measured by Dr. G. Andreev (EVS Co)

Single pass AFM, KPFM, and Reflection of self assembled alkane nanostructures on Si

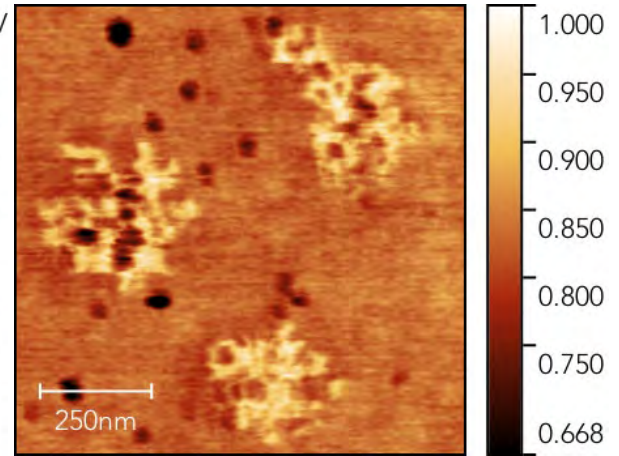
Height



Surface Potential

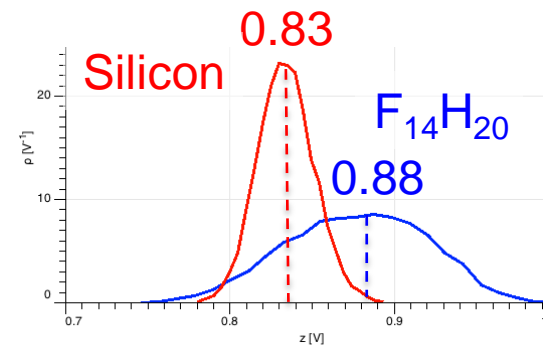


Re(Refl.) $\lambda=10.6\mu\text{m}$

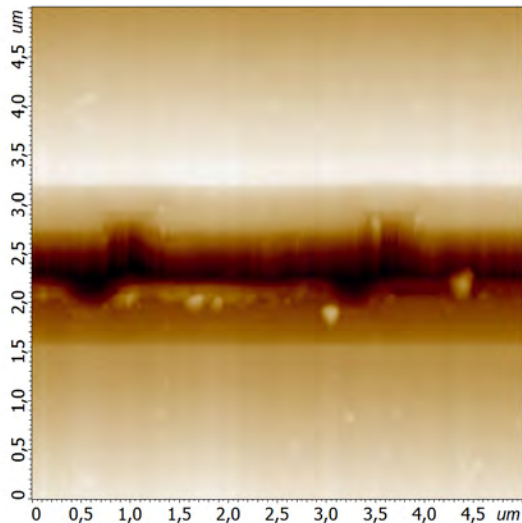


- Simultaneous nanoscale electrical and optical properties measured for the first time
- Reflection contrast of thin and soft structures easily detectable
- Better than $\lambda/1000$ spatial resolution

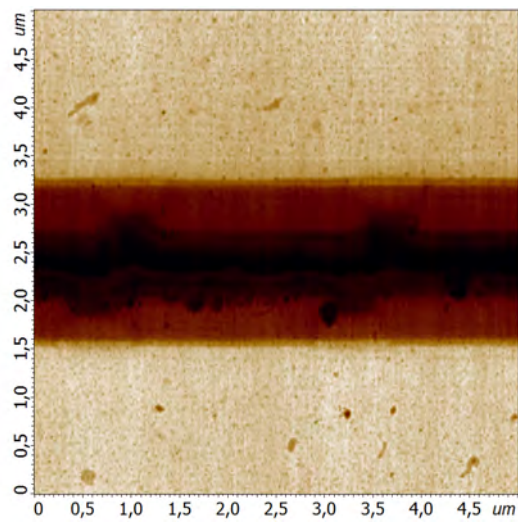
Reflection Distribution



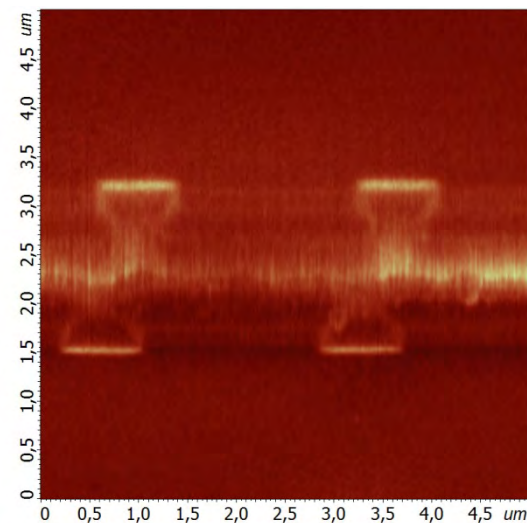
p-doped Si grating



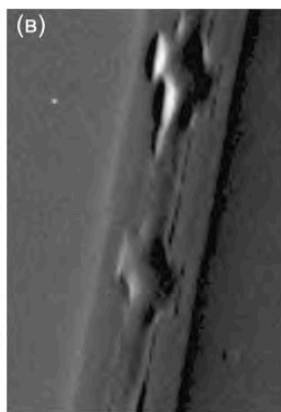
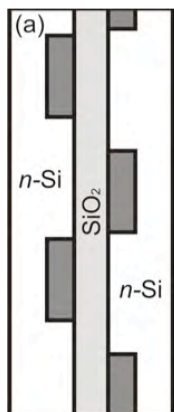
AFM topography



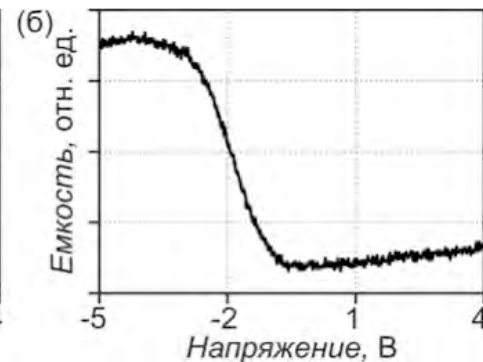
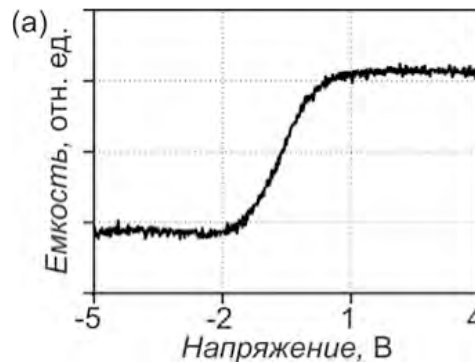
s-SNOM signal, Amplitude



s-SNOM signal, Phase



(a) – sample structure, (b) – capacitance contrast dC/dV , (B) – topography (*measured separately*)
Scan size 3.5x5 μm

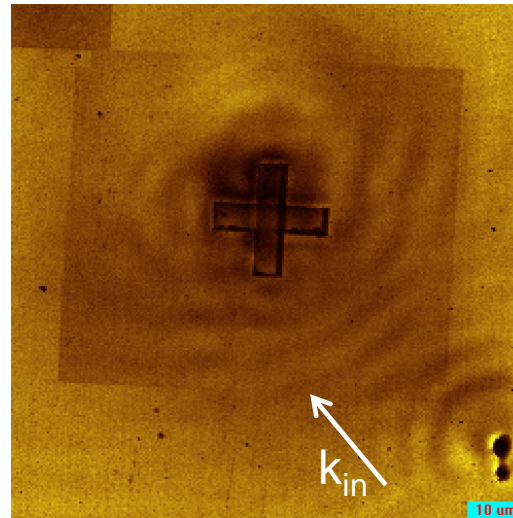


C-V curves measured on the wafer (right) and in the doped region (left)

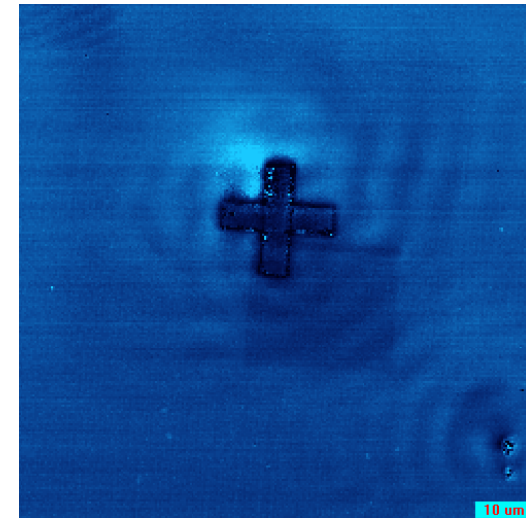
Interference of optical surface waves in SiC



AFM topography



Near-field Amplitude



Near-field Phase

Interference of optical surface waves (propagating Surface Phonon Polaritons, SPhP) at the surface of SiC crystal is observed in Amplitude and Phase near-field optical images. The surface waves are excited by CO₂ laser plane wave directed from the bottom-right (k_{in}). SPhP wave beating pattern caused by presence of surface features is observed.

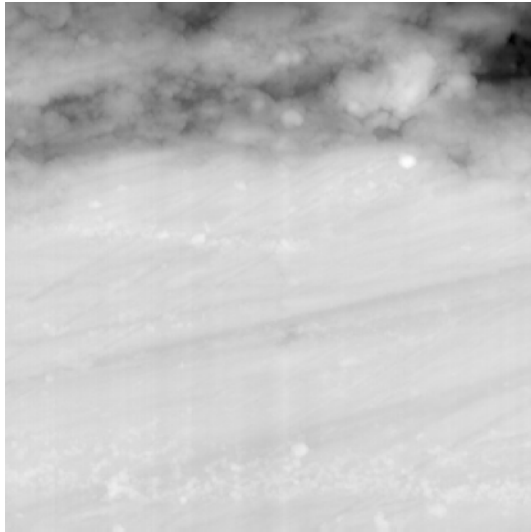
Sample: SiC crystal with etched cross-like structure on the surface

Excitation laser: 10.8 μm (923 cm^{-1})

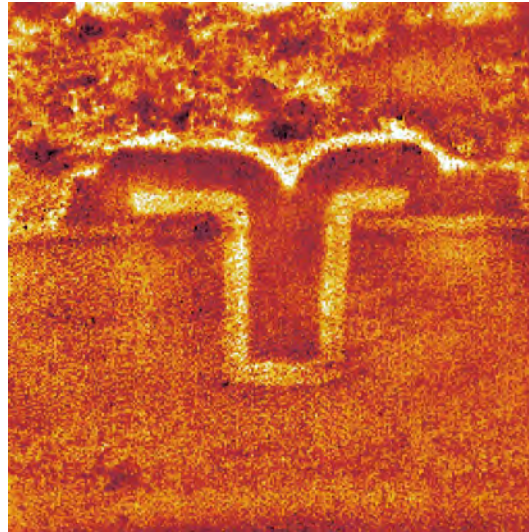
Measurement mode: s-SNOM optical signal (Amplitude and Phase) by interferometric homodyning

Image size: 90x90 μm

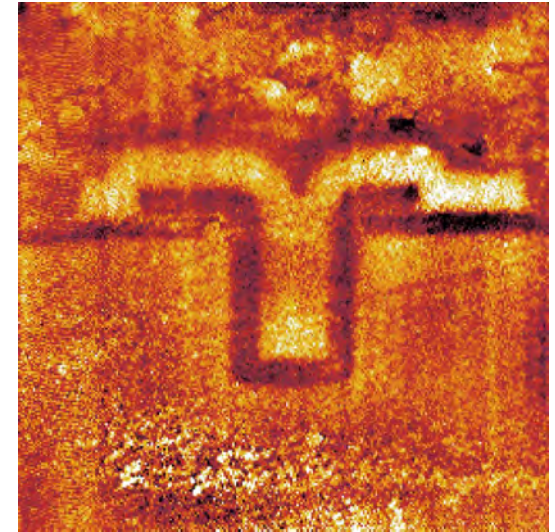
MOS transistor mapping, material and doping contrast



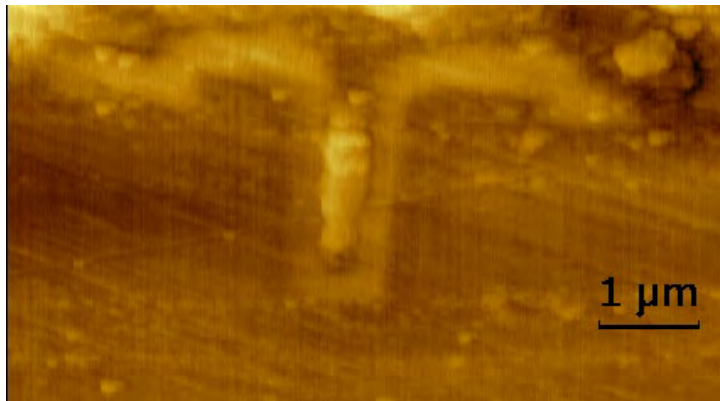
AFM topography



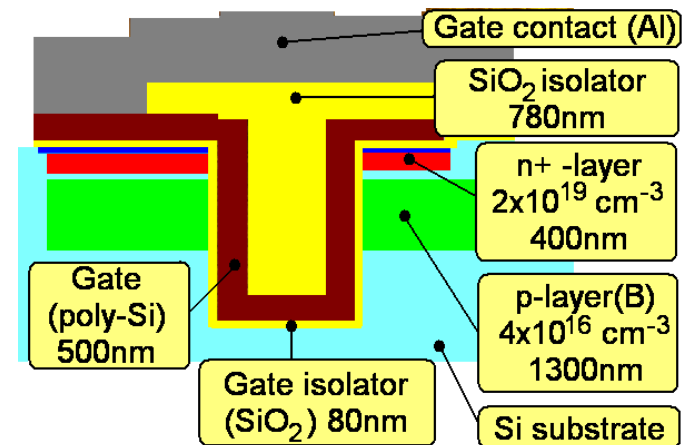
s-SNOM signal, Amplitude



s-SNOM signal, Phase



Kelvin probe microscopy, surface potential
(*measured separately*)

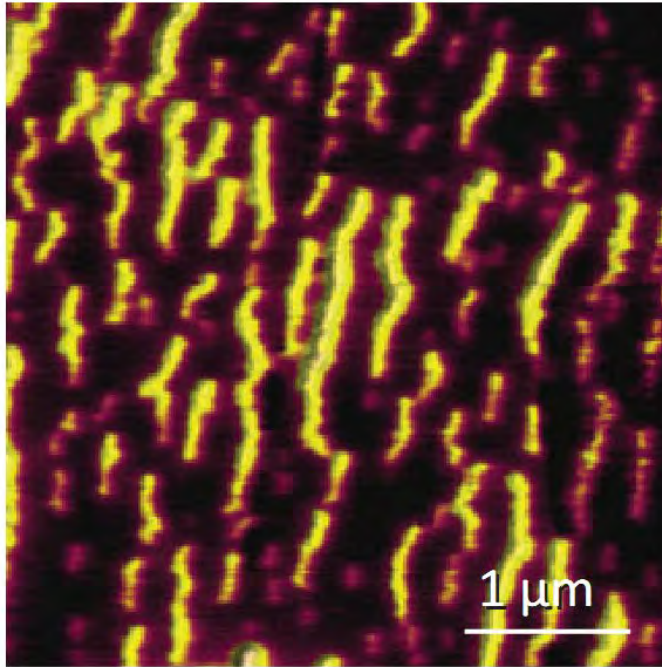


Sample: Si trench defined MOS transistor. Excitation laser: 10.8 μm (923 cm⁻¹). Image size: 10x10 μm
Measurement mode: s-SNOM optical signal (Amplitude and Phase) by interferometric homodyning

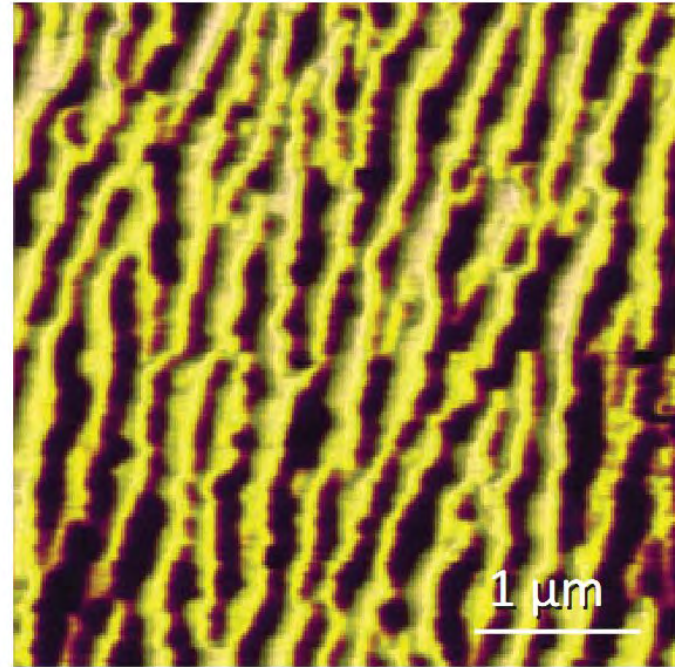
sSNOM on a phase changing material: VO₂

IR sSNOM Reflection

27C

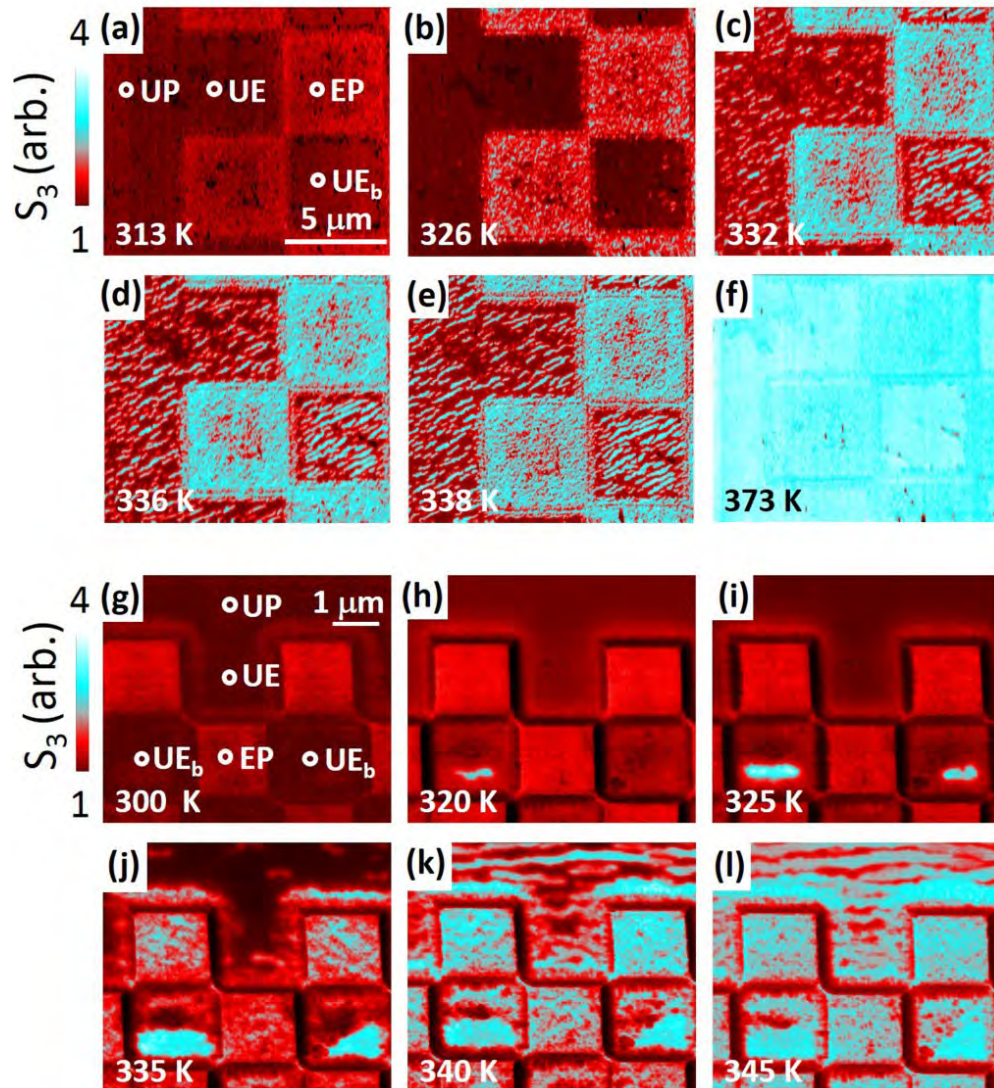


67C



Superior high temperature performance: <1 hour needed to acquire images 40C apart. Low drift and high signal stability: <1μm XY drift from 27 to 67C, no realignment of nanoReflection optics needed
Sample courtesy to prof. Liu (Stony Brook University, New York, USA)

IR s-SNOM: VO₂ Thin Films



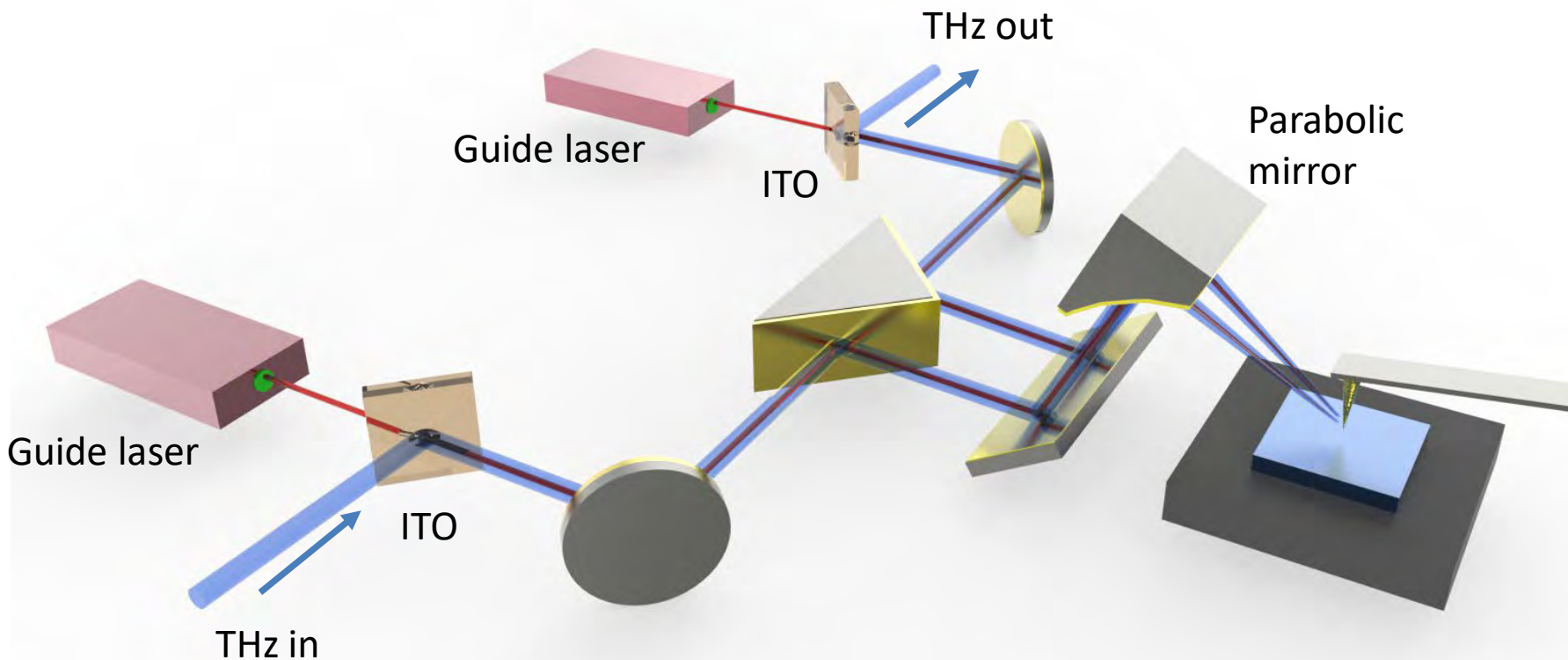
Temperature-dependent infrared near-field images of patterned VO₂/TiO₂ at 11 μm , revealing area-dependent insulator-to-metal phase transitions.

The metallic phase is shown in cyan and the insulating phase is in red.

(a)–(f) 5 $\mu\text{m} \times 5 \mu\text{m}$ checkerboard patterns at (a) 313, (b) 326, (c) 332, (d) 336, (e) 338, and (f) 373 K.

(g)–(l) 1.5 $\mu\text{m} \times 1.5 \mu\text{m}$ checkerboard patterns on the same sample, at (g) 300, (h) 320, (i) 325, (j) 335, (k) 345, and (l) 350 K. The smaller scale of the pattern shown in (g)–(l) exhibits strain-induced confinement effects, especially in the fully bounded UE regions (UE_b).

THz s-SNOM



THz s-SNOM: Nanoimaging of graphene

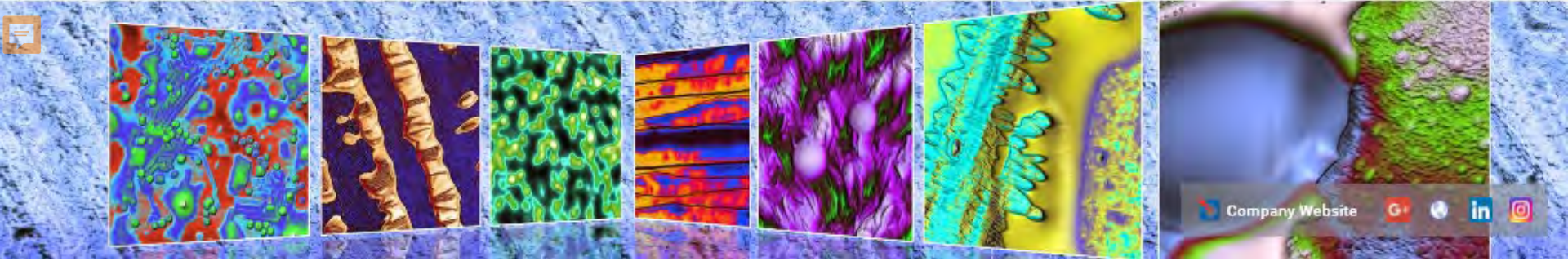
(black).

ized S_2 spectra of graphene (red) and SiO_2



Thank you for your attention!

www.ntmdt-si.com



Follow us in social networks!
#NTMDT

